Basic Res Cardiol (2017) 112:24
DOI 10.1007/s00395-017-0613-6

ORIGINAL CONTRIBUTION

Cavin-1 deficiency modifies myocardial and coronary function, stretch responses and ischaemic tolerance: roles of NOS over-activity

Mika Kaakinen[1,2] · Melissa E. Reichelt[3] · Zhibin Ma[3] · Charles Ferguson[2] · Nick Martel[2] · Enzo R. Porrello[3] · James E. Hudson[3] · Walter G. Thomas[3] · Robert G. Parton[2] · John P. Headrick[4]

Received: 14 December 2016 / Revised: 9 February 2017 / Accepted: 9 March 2017 / Published online: 25 March 2017

Abstract Caveolae and associated cavin and caveolins may govern myocardial function, together with responses to mechanical and ischaemic stresses. Abnormalities in these proteins are also implicated in different cardiovascular disorders. However, specific roles of the cavin-1 protein in cardiac and coronary responses to mechanical/metabolic perturbation remain unclear. We characterised cardiovascular impacts of cavin-1 deficiency, comparing myocardial and coronary phenotypes and responses to stretch and ischaemia–reperfusion in hearts from *cavin-1*$^{+/+}$ and *cavin-1*$^{-/-}$ mice. Caveolae and caveolins 1 and 3 were depleted in *cavin-1*$^{-/-}$ hearts. Cardiac ejection properties in situ were modestly reduced in *cavin-1*$^{-/-}$ mice. While peak contractile performance in ex vivo myocardium from *cavin-1*$^{-/-}$ and *cavin-1*$^{+/+}$ mice was comparable, intrinsic beating rate, diastolic stiffness and Frank–Starling behaviour (stretch-dependent diastolic and systolic forces) were exaggerated in *cavin-1*$^{-/-}$ hearts. Increases in stretch-dependent forces were countered by NOS inhibition (100 μM L-NAME), which exposed negative inotropy in *cavin-1*$^{-/-}$ hearts, and were mimicked by 100 μM nitroprusside. In contrast, chronotropic differences appeared largely NOS-independent. Cavin-1 deletion also induced NOS-dependent coronary dilatation, ≥3-fold prolongation of reactive hyperaemic responses, and exaggerated pressure-dependence of coronary flow. Stretch-dependent efflux of lactate dehydrogenase and cardiac troponin I was increased and induction of brain natriuretic peptide and c-Fos inhibited in *cavin-1*$^{-/-}$ hearts, while ERK1/2 phospho-activation was preserved. Post-ischaemic dysfunction and damage was also exaggerated in *cavin-1*$^{-/-}$ hearts. Diverse effects of cavin-1 deletion reveal important roles in both NOS-dependent and -independent control of cardiac and coronary functions, together with governing sarcolemmal fragility and myocardial responses to stretch and ischaemia.

Keywords Caveolar proteins · Cardiac compliance · Reactive hyperaemia · Ischaemia–reperfusion · Nitric oxide synthase · Membrane permeability · Stretch-response

Introduction

The plasma membrane of most cells is decorated with tiny flask-like caves, termed caveolae. In addition to single pits, caveolae may form extensive networks of interconnected structures that have been termed rosettes [58]. Caveolae and their coat proteins regulate membrane receptor, ion channel and transporter functions, are key to stretch-dependent

Electronic supplementary material The online version of this article (doi:10.1007/s00395-017-0613-6) contains supplementary material, which is available to authorized users.

Mika Kaakinen, Melissa E. Reichelt, Robert G. Parton and John P. Headrick contributed equally.

✉ Robert G. Parton
R.Parton@imb.uq.edu.au

✉ John P. Headrick
J.Headrick@griffith.edu.au

[1] Oulu Center for Cell-Matrix Research, Faculty of Biochemistry and Molecular Medicine, Biocenter Oulu, University of Oulu, Oulu, Finland

[2] Institute for Molecular Biosciences, The University of Queensland, St Lucia, QLD 4072, Australia

[3] School of Biomedical Sciences, The University of Queensland, Brisbane, Australia

[4] School of Medical Science, Griffith University, Southport, QLD 4217, Australia

signalling/mechanotransduction, and confer resistance to mechanical [70] and ischaemic insults [84, 111]. Caveolin-1 or muscle-specific caveolin-3 are major structural elements, incorporating into the inner leaflet of the membrane with the aid of hairpin loop structures. Initially identified as a regulator of transcription termination [50], cavin-1 (or PTRF) coats the cytoplasmic surface of caveolae where it stabilises caveolins and is essential for caveola formation and morphology [7, 46]. Via hetero-oligomerisation with other cavins [35, 56], cavin-1 helps assemble a complex of cavin proteins on the cytoplasmic face of plasma membrane caveolae [7]. Accordingly, cavin-1 deficiency results in depression of cavin-2 and -3 in cardiac and skeletal muscle, while cavin-4 (also known as muscle specific coiled coil protein, MURC) is reduced in heart [57, 94]. The inducibility of cavin-1 with differing stressors [1, 100] may also provide for stress-sensitivity of caveolar formation. However, the specific myocardial and coronary functions of cavin-1 remain to be fully elucidated. Mutations in the cavin-1 protein are associated with fatal cardiac arrhythmia, long-QT syndrome [77] and muscular dystrophy [43], coupled with abnormal localisation of caveolins.

As for caveolin-1 or -3, deletion of cavin-1 eliminates caveolae in association with caveolin destabilisation/degradation [57]. Nonetheless, cavin-1 may exert effects distinct from those of caveolins. In contrast to caveolin-3 [42, 98] and cavin-4 [83], cardiac hypertrophy is not evident in carriers of cavin-1 mutations. Similarly, while caveolin-3 knockout induces hypertrophy (akin to caveolin-3 mutation carriers) [107], and caveolin-1 deletion induces cardiomyopathy [21, 114], these changes are not consistently observed with cavin-1 deletion. The limited studies of *cavin-1*$^{-/-}$ mice report: metabolic changes that include resistance to dietary obesity, altered lipid metabolism, glucose intolerance and hyperinsulinaemia [29, 57]; cardiovascular changes, including exaggerated vasoconstriction and impaired vasomotion and autoregulation [91], and pulmonary hypertension/remodelling with associated right ventricular hypertrophy [92]; and contractile dysfunction/hypertrophy in non-vascular smooth muscle [52]. Cardiac hypertrophy, dysfunction and ECG abnormalities were also very recently reported in the hearts of female *cavin-1*$^{-/-}$ mice [94]. Distinct from prior observations [29, 52, 57], this recent study also reported a substantial reduction in body weight with cavin-1 deletion. Given the limited and mixed data regarding effects of cavin-1 deletion on cardiovascular phenotype, we undertook the first detailed analysis of both myocardial and coronary phenotypes in *cavin-1*$^{-/-}$ mice, including myocardial structure, cardiac and coronary function and responses to mechanical and ischaemic stressors, stretch-dependent myocardial signalling, and plasma membrane fragility or permeability.

Methods

Mouse model

Cavin-1$^{-/-}$ mice (C57Bl/6 strain) were obtained from Boston University School of Medicine [57]. To improve breeding and animal survival [19] *cavin-1*$^{-/-}$ males were mated with wild-type females from a CD-1 background. Resulting heterozygous F1 generation mice were mated with unrelated F1 mice to generate *cavin-1*$^{-/-}$ and *cavin-1*$^{+/+}$ CD-1/C57Bl/6 hybrids. Approximately equal numbers of male and female offspring were evident in litters, with data presented in the study pooled for both sexes. Structural and functional data segregated according to sex are included in the Data Supplement.

Echocardiography, electrocardiography and morphometry

Echocardiographic examinations were performed in 2-month-old (mo) mice under 2.5% isoflurane anaesthesia on a heat mat. M-wave recordings of the parasternal short axis of the left ventricle were performed using a Philips HD15 ultrasound unit and high-frequency (15 MHz linear array transducer) probe (Philips; Amsterdam, The Netherlands). Electrocardiographic (ECG) examination was performed under Ketamine (10 mg/mL) and Xylazil (1.6 mg/mL) anaesthesia, using a FE-136 Bio Amp connected to a 4/25 Powerlab (ADInstruments Pty Ltd., Bella Vista, Australia). Signals were filtered (10 Hz high pass, 200 Hz low pass, 50 Hz notch filters) and ECG data analysed over 30 s of steady state recordings (data presented as mean of five measures). For morphometric analysis, mice were weighed and killed by cervical dislocation. Hearts were excised, rinsed in phosphate buffered saline, blotted and weighed. Tibial length was measured and used for normalisation of heart weight.

Histology and microscopy

Hearts were excised from killed animals and immediately immersed in 10% formalin for a minimum of 12 h. Fixed hearts were washed 30 min with PBS and immersed in 70% ethanol until processed for histological sectioning. Paraffin sections (4 μm) were stained with hematoxylin and eosin (H&E) and Masson's trichrome. Histological procedures were conducted by the QIMR Berghofer MRI Histology Services at the Royal Brisbane Hospital Queensland. For electron microscopy, rapidly dissected tissue pieces were fixed by perfusion with 2.5% glutaraldehyde in PBS and processed for Epon embedding, as described previously [93]. Ultrathin sections were viewed

in a Jeol (Tokyo, Japan) 1011 transmission electron microscope and imaged using the iTEM analysis program (Soft Imaging System, Muenster, Germany).

Langendorff heart model

Hearts were isolated from age-matched *cavin-1*$^{-/-}$ or *cavin-1*$^{+/+}$ (wild-type) mice, and perfused as detailed previously [81, 88]. Unless otherwise stated, both male and females were studied and data pooled. After measurement of body weight, mice were anaesthetised with 10 mg/mL ketamine and 1.6 mg/mL xylazil (i.p.) and hearts isolated and perfused in a Langendorff mode at a coronary pressure of 80 mmHg with modified Krebs–Henseleit buffer containing (in mM): NaCl, 119; $NaHCO_3$, 22; KCl, 4.7, $MgCl_2$, 1.2; KH_2PO_4, 1.2; EDTA, 0.5; $CaCl_2$, 1.85; D-(+)-glucose, 11; and Na^+-pyruvate, 2 (all from Sigma Aldrich, St. Louis, MO, USA), bubbled with 95% O_2/5% CO_2 to maintain pH at 7.4 at 37 °C. Contractile function was measured via a fluid-filled plastic film ventricular balloon connected to a pressure transducer, and coronary flow measured via an in-line Doppler flow probe (Transonic Systems Inc., Clifton, NJ, USA), with data recorded on a four-channel MacLab system (ADInstruments Pty Ltd.; Bella Vista, Australia) [81, 88]. After preparation, hearts were immersed in a 5-mL water jacketed chamber (37 °C), with perfusion fluid and chamber temperatures monitored via needle thermistors.

Ventricular pressure–volume relationships

Ventricular pressure–volume relationships (PVRs) were assessed in hearts (equal mass of ~160 mg) from 5 to 6 months old *cavin-1*$^{-/-}$ and *cavin-1*$^{+/+}$ mice. After instrumentation, the ventricular balloon was briefly inflated to yield a systolic pressure of ~100 mmHg before adjusting volume to maintain systolic pressure at zero over a 10 min stabilisation period. Hearts were paced where necessary to maintain a mean rate of 470 beats/min across groups. After stabilisation at zero systolic pressure, balloon volume was incrementally increased in 2.65 µL steps using a 500-µL threaded syringe (Hamilton Co; Reno, NV, USA) and function assessed after 2 min at each volume. Experiments were terminated when end-diastolic pressure exceeded 30 mmHg. Analyses were undertaken in hearts either untreated or treated with 100 µM of the NOS inhibitor L-NAME (Sigma Aldrich; St. Louis, MO, USA). A subset of *cavin-1*$^{+/+}$ hearts were treated with a high 100 µM concentration of the NO donor sodium nitroprusside (SNP) to identify the acute functional impacts of excessive NO generation.

Coronary phenotype

For assessment of coronary vascular phenotype, a series of analyses were performed in hearts from 5 to 6 months *cavin-1*$^{-/-}$ and *cavin-1*$^{+/+}$ mice. Basal coronary flow was measured in hearts performing minimal work (un-inflated balloons) and during incremental increases in volume-dependent contractile function (functional hyperaemia) in PVR studies. Influences of diastolic compression on coronary perfusion were also estimated from the relation between end-diastolic pressure and flow in *cavin-1*$^{+/+}$ hearts treated with SNP (maximally dilated) and subjected to ventricular volume loading. To assess coronary reactive hyperaemic responses, hearts were stabilised for 20 min (ventricular balloon un-inflated) before assessing coronary responses to 10, 20 or 30 s occlusions (5 min recovery period between each). Experiments were performed in untreated hearts and hearts receiving 100 µM L-NAME, initiated after 15 min stabilisation. The relation between coronary flow and perfusion pressure (reflecting autoregulatory or myogenic function) was briefly assessed from hearts perfused at flows of either 1 or 3 mL/min.

Myocardial ischaemia–reperfusion

Perfused hearts from 2 mo *cavin-1*$^{-/-}$ and *cavin-1*$^{+/+}$ mice were initially allowed to beat at intrinsic rates for 15 min before pacing at 430 beats/min. After a further 15 min stabilisation, global normothermic ischaemia was induced for 25 min followed by 45 min aerobic reperfusion. Coronary effluent collected prior to ischaemia and throughout reperfusion was stored on ice or at −70 °C until assayed for release of lactate dehydrogenase (LDH) and cardiac troponin I (cTnI).

Analysis of myocardial LDH and TnI efflux

Coronary venous levels of LDH were assessed using a Cytotoxicity Detection Kit-Plus (Roche; Basel, Switzerland), according to manufacturer's instructions. Samples were assayed in duplicate, with efflux (U/min) normalised to estimated heart weight. Myocardial release of cTnI was assessed via ELISA (LifeDiagnostics, Inc.; West Chester, PA, USA): coronary effluent samples were thawed in an ice bath and assayed for cTnI according to manufacturer instructions. Optical density was determined spectrophotometrically at 450 nM and cTnI efflux rates normalised to heart weight.

Cardiac stretch responses and membrane leakage/fragility

To assess stretch-dependent protein efflux and cell signalling responses, hearts from *cavin-1*$^{-/-}$ and *cavin-1*$^{+/+}$ mice were stabilised at a coronary pressure of 80 mmHg

before switching to either low- (1 mL/min) or high-flow (3 mL/min) perfusion. Coronary efflux of LDH was assessed over 2 h, before dissecting hearts into three portions in ice-cold Krebs–Henseleit buffer and freezing in liquid N_2 for subsequent molecular analyses.

To examine membrane permeability or fragility, a series of hearts were perfused at 1 mL/min for 10 min before infusing a 10% Evans blue solution (w/v in Krebs–Henseleit buffer, filtered through a 0.22 μm filter) at 20 μL/min for 1 min, followed by a 10 min wash to rid excess stain. Hearts were frozen in liquid N_2 cooled isopentane and stored at −70 °C until analysis. Frozen heart samples were sliced into 10 μm sections with a cryomicrotome (Leica; Wetzlar, Germany). Evans blue treated tissue was imaged immediately after sectioning and fixed thereafter for 10 min with 4% paraformaldehyde in PBS. Cell membranes were solubilised with 1% Triton-X100 in PBS for 5 min followed by blocking of unspecific staining with 1% BSA in PBS for 10 min. Sections were incubated with rat anti-CD31 antibody (BD Biosciences; Franklin Lakes, NJ, USA) for 30 min at 37 °C. After three washes with PBS (10 min) the antibody was detected with Alexa 488 conjugated anti-rat secondary antibody for 30 min at 37 °C. The sections were counterstained for the nuclear marker DAPI.

Western immunoblotting

Lateral left ventricular wall was homogenised (IKA T-10 Basic homogeniser) in buffer containing 50 mM Tris (pH 8), 150 mM NaCl, 1% Triton-X 100, 0.1% SDS, 5 mM EDTA, and Complete protease and PhosStop phosphatase inhibitors (Roche; Basel, Switzerland). Homogenates were sonicated 4 × 10 s with a VirSonic 100 ultrasonic cell disrupter (VirSonic; Woburn, MA, USA) and centrifuged at 2000×*g* for 2 min. Protein concentration was measured using a colorimetric BCA assay (Thermo Scientific; Waltham, MA, USA). Equal amounts of protein were then loaded onto 10% acrylamide gels. Proteins were transferred to LF-PVDF membranes and blocked in 5% BSA in Tween-20 Tris buffered saline (TBST) for 60 min before incubation overnight (at 4 °C) with specific antibodies in 5% BSA: from Sigma Aldrich (St. Louis, MO, USA), tubulin (T9026); from BD Biosciences (NJ, USA), caveolin-3 (#610421), caveolin-1 (#610060), eNOS/NOS Type III (#610296) and rat CD-31 (#550274); and from Cell Signaling Technology (Danvers, MA, USA), total and phosphorylated p38-MAPK (#92112,#9212), c-Jun NH2-terminal protein kinase (JNK; #9252S, #4668S), AKT (#9272, #4060) and ERK (#9102S, #9101S). Following washing, membranes were incubated for 1 h with horseradish peroxidase conjugated secondary antibody (anti-rabbit or anti mouse; Sigma Aldrich) diluted with 5% non-fat milk in TBST. Detection was achieved using Clarity™ Western ECL substrate with bands visualised using a ChemiDoc™ Imaging system (Bio-Rad; Hercules, CA, USA).

Quantitative RT PCR

Samples were prepared using a Qiagen RNAeasy Minikit according to manufacturer protocol. Genomic DNA was digested with RNase-free DNase (Qiagen; Hilden, Germany), and cDNA generated using Superscript™ III first strand synthesis (Invitrogen; Carlsbad, CA, USA) and random primers. Quantitative PCR was performed using a ViiATM 7 RT PCR using SYBR® Green (Applied Biosystems; Waltham, MA, USA) as a detection system and gene specific primers for: mouse c-Fos (forward 5′-CGGGTTTCAACGCCGACTA-3′; reverse 5′-TTGGCACTAGAGACGGACAGA-3′); HPRT1 (forward 5′-TGGATACAGGCCAGACTTTG-3′; reverse 5′-CGTGATTCAAATCCCTGAAG-3′); and brain natriuretic peptide (BNP) (forward 5′-TGGGCACAAGATAGACCG GA-3′; reverse 5′-CAACTTCAGTGCGTTACAGC-3′). Quantification of PCR products was performed using the $2^{\Delta\Delta C_T}$ method.

Statistics

Values are mean ± SEM. When appropriate, Grubbs' test was used to identify outliers. An *F* test was used to compare variances. Paired/unpaired *t* tests, Mann–Whitney *U* tests (for unequal variances in unpaired samples) or Kruskal–Wallis test (for unequal variances in unpaired multi-group samples) were used for comparisons. For multivariable analysis two-way ANOVA with repeated measures followed by Sidak's post hoc testing was employed. An 'area under the curve' (AUC) analysis was applied to contrast PV responses (Fig. 2), while to detail specific differences in PV data we contrasted hearts with a full complement of data from 0 to 21.2 μL volumes via ANOVA and Sidak's post hoc test ($n = 11$, 8, 13 and 6 for *cavin-1*$^{+/+}$, *cavin-1*$^{-/-}$, *cavin-1*$^{+/+}$+ L-NAME and *cavin-1*$^{-/-}$ + L-NAME, respectively). Linear regression was used to evaluate relationships between coronary flow and systolic pressure. In all tests a $P < 0.05$ was considered significant, with all analyses performed using Prism 7 (GraphPad Software, Inc; San Diego, Ca, USA).

Results

Genetic loss of cavin-1 depletes caveolae and caveolins without otherwise causing structural changes

Microscopic inspection confirmed depletion of caveolae in myocardial tissue from *cavin-1*$^{-/-}$ mice (Fig. 1, upper

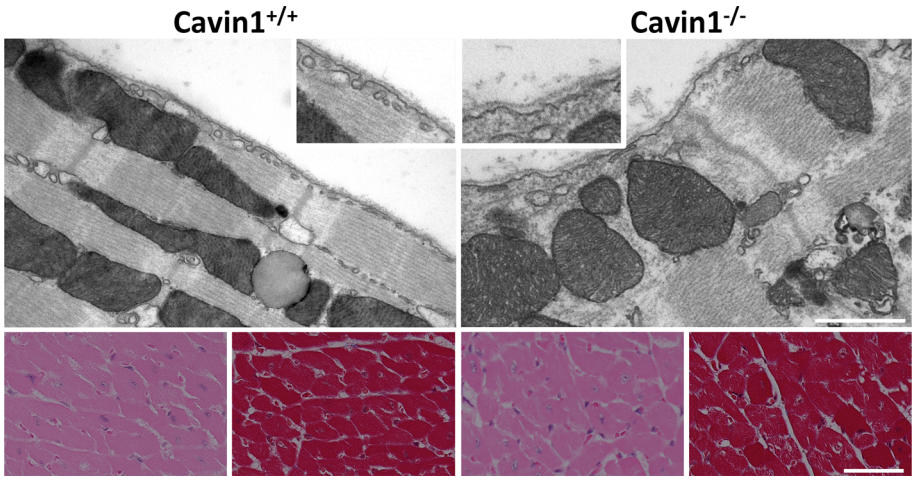

Fig. 1 Hearts from *cavin-1*$^{-/-}$ mice exhibit depletion of caveolae without fibrosis. *Top* Transmission electron micrographs of cardiac myocytes from *cavin-1*$^{+/+}$ (*left*) and *cavin-1*$^{-/-}$ mice (*right*), including magnified sections (*boxes*). Caveolae localise to the sarcolemma of cardiomyocytes in *cavin-1*$^{+/+}$ hearts, while the plasma membrane of *cavin-1*$^{-/-}$ cardiomyocytes appears devoid of caveolae. *Scale bar* 1 μM. *Bottom* Histological sections from *cavin-1*$^{+/+}$ (*left*) and *cavin-1*$^{-/-}$ mice (*right*), stained with Masson trichrome and H&E, respectively. *Scale bar* 50 μm

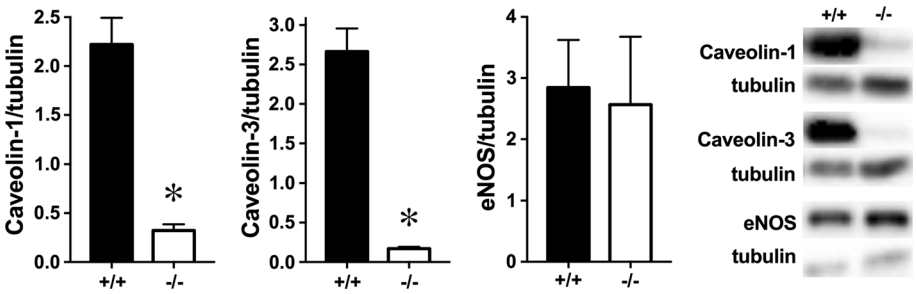

Fig. 2 Caveolin-1 and caveolin-3 levels are depressed in hearts from *cavin-1*$^{-/-}$ mice. Myocardial expression of caveolin-1, caveolin-3 and eNOS was assessed and normalised to β-tubulin in *cavin-1*$^{+/+}$ (+/+, $n = 3$) and *cavin-1*$^{-/-}$ (−/−, $n = 3$) hearts. Cavin-1 deletion significantly reduces caveolin-1 and caveolin-3 expression without altering total eNOS levels. Immunoblot images are provided in the Data Supplement (Fig. S1). Data are mean ± SEM. *$P < 0.05$ vs. *cavin-1*$^{+/+}$

panels). There was no evidence of structural changes or fibrosis in *cavin-1*$^{-/-}$ hearts, as shown in Masson's trichrome and H&E stained sections (Fig. 1, lower panels). Hearts of *cavin-1*$^{-/-}$ mice also expressed reduced levels of both caveolin-1 and caveolin-3 protein (Fig. 2; Fig. S1), consistent with prior observations [57, 94]. In contrast, cardiac expression of eNOS, a key enzyme regulated by caveolae and caveolins, was unaltered with cavin-1 deletion (Fig. 2; Fig. S1).

Cavin-1 deletion has limited impacts on cardiac morphology while depressing in vivo function at 2 months of age

Transthoracic echocardiography and morphometric analyses in 2 months mice revealed a modest 10% increase in cardiac mass normalised to body weight without significantly influencing ventricular wall thickness (Table 1). Cardiac ejection properties was also depressed, with a 10% fall in ejection fraction and 20% fall in fractional shortening (Table 1). Results detailed in the Data Supplement hint at potentially greater inhibitory effects of cavin-1 deletion in females vs. males (Table S1). Electrocardiographic analysis in vivo revealed no major rate or waveform differences in *cavin-1*$^{-/-}$ vs. *cavin-1*$^{+/+}$ hearts (Table 1).

Impact of cavin-1 deletion on ex vivo myocardial function

Baseline contractile function ex vivo did not differ between hearts from 2 or 5–6 mo *cavin-1*$^{-/-}$ and *cavin-1*$^{+/+}$ mice (Table 2), and was similar in males and females (Table S2). However, intrinsic heart rate was increased in *cavin-1*$^{-/-}$ hearts (Table 2), a 60–65 beat/min elevation that was not eliminated by NOS inhibition (which reduced

Table 1 Morphometric, echocardiographic and electrocardiographic parameters in *cavin-1*$^{+/+}$ and *cavin-1*$^{-/-}$ mice

Parameter	*Cavin-1*$^{+/+}$	*Cavin-1*$^{-/-}$
Body weight (g)	28.6 ± 0.6 (n = 22)	27.5 ± 0.7 (n = 24)
$\frac{\text{Bodyweight}}{\text{Tibial length}}$ (g/mm)	1.60 ± 0.03 (n = 22)	1.60 ± 0.04 (n = 22)
Heart weight (mg)	150.7 ± 7.3 (n = 12)	140.2 ± 5.9 (n = 12)
$\frac{\text{Heartweight}}{\text{Body weight}}$	0.0050 ± 0.0002 (n = 11)	0.0056 ± 0.0001 (n = 12)*
Ejection fraction (%)	81.3 ± 2.4 (n = 9)	72.1 ± 2.3 (n = 11)*
Fractional shortening (%)	43.7 ± 2.5 (n = 9)	35.2 ± 1.9 (n = 4)*
$LVPDW_d$ (mm)	0.99 ± 0.03 (n = 9)	0.90 ± 0.02 (n = 11)
IVS_d (mm)	0.81 ± 0.03 (n = 9)	0.79 ± 0.03 (n = 11)
ECG: RR (s)	0.167 ± 0.014 (n = 15)	0.164 ± 0.015 (n = 16)
ECG: RP (s)	0.176 ± 0.051 (n = 11)	0.119 ± 0.023(n = 9)
ECG: QT/RR	0.537 ± 0.028 (n = 8)	0.543 ± 0.047 (n = 10)

Data were acquired from 2 months male and female mice. Values are mean ± SEM

$LVDW_d$ left ventricular wall thickness during diastole, *IVS_d* inter-ventricular thickness during diastole. For symbols RR, RP and QT/RR see Fig. S1

* $P < 0.05$; *** $P < 0.005$ (vs. *cavin-1*$^{+/+}$)

heart rates 25–40 beat/min). The *cavin-1*$^{-/-}$ hearts also appeared more arrhythmic (Fig. S2). This was more apparent in females (6/13 *cavin-1*$^{-/-}$ vs. 1/13 *cavin-1*$^{+/+}$ hearts) than males (2/8 *cavin-1*$^{-/-}$ vs. 1/7 *cavin-1*$^{+/+}$ hearts).

NO-dependent diastolic stiffness, and NO-dependent and independent contractile changes in hearts of *cavin-1*$^{-/-}$ mice

Stretch dependencies of diastolic force (stiffness or compliance) and active force development (Frank–Starling response) were assessed in *cavin-1*$^{+/+}$ and *cavin-1*$^{-/-}$ hearts (cardiac masses 159 ± 7 and 159 ± 5 mg, respectively). *Cavin-1*$^{-/-}$ hearts displayed a substantial leftward shift of the diastolic PVR (Fig. 3a), evident in males and females (Fig. S3). The initial phase of the PVR appeared steeper in *cavin-1*$^{-/-}$ hearts, linear regression identifying a greater initial slope (1.69 ± 0.08 mmHg/μL between 2.65–10.58 μL). Further volume changes more modestly impacted diastolic pressure (slope 0.66 ± 0.10). Diastolic pressure increased relatively linearly with volume in *cavin-1*$^{+/+}$ hearts (slope 0.37 ± 0.06). The systolic PVR also shifted to lower volumes in *cavin-1*$^{-/-}$ hearts (Fig. 3b), suggesting positive inotropy, an effect more prominent in females (Fig. S3). Nonetheless, peak systolic and developed pressures were equivalent in *cavin-1*$^{+/+}$ and *cavin-1*$^{-/-}$ hearts (Fig. 3b, c; Table 2).

Since cavin-1 deletion suppresses expression of caveolin-1 (Fig. 2) [57, 94], a key inhibitor of eNOS, and NOS/NO influences contractility/compliance, we tested effects of NOS inhibition. Total eNOS expression was confirmed as comparable in both *cavin-1*$^{-/-}$ and *cavin-1*$^{+/+}$ hearts (Fig. 2). Infusing L-NAME shifted the diastolic PVR in *cavin-1*$^{-/-}$ (not *cavin-1*$^{+/+}$) hearts, eliminating compliance differences between groups (Fig. 3a). Additionally, L-NAME reduced contractile function in *cavin-1*$^{-/-}$ but not *cavin-1*$^{+/+}$ hearts, right-shifting the systolic PVR to expose NOS-independent negative inotropy (Fig. 3b), a change that may also be more pronounced in females (Fig. S3). Moreover, SNP left-shifted the diastolic PVR in *cavin-1*$^{+/+}$ hearts (Fig. 3d), resembling effects of cavin-1 deletion (including steeper diastolic PVR: slope 1.36 ± 0.07 from 2.65 to 10.58 μL volumes vs. 1.69 ± 0.08 in *cavin-1*$^{-/-}$ hearts). The systolic PVR was also significantly shifted with SNP.

Increased coronary flow and reactive hyperaemia duration via NOS activity in hearts of *cavin-1*$^{-/-}$ mice

Baseline coronary flow was significantly increased with cavin-1 deletion, an effect prominent in hearts performing minimal pressure work (Fig. 4a, b). This baseline flow difference dissipates as ventricular pressure development is increased (Fig. 4c), reflecting a functional (metabolic) hyperaemia in *cavin-1*$^{+/+}$ hearts that appears obviated by baseline vasodilatation in *cavin-1*$^{-/-}$ hearts (Fig. 4c). Dependence of coronary flow on pressure also appeared exaggerated in hearts of *cavin-1*$^{-/-}$ mice (Fig. S4A), suggesting impaired myogenic control. Reactive hyperaemia was modified, with cavin-1 deletion prolonging hyperaemic durations without altering peak flows (Fig. 4a, b). A 'shoulder' or secondary dilatation was also evident 10–15 s after peak hyperaemia in *cavin-1*$^{-/-}$ hearts (Fig. 4a). Actual flow 'debt' was moderately increased in

Table 2 Baseline functional parameters for Langendorff-perfused hearts from *cavin-1*$^{+/+}$ and *cavin-1*$^{-/-}$ mice

	2 months (baseline)		5–6 months (peak function)			
	Cavin-1$^{+/+}$	*Cavin-1*$^{-/-}$	Untreated		+100 μM L-NAME	
			Cavin-1$^{+/+}$	*Cavin-1*$^{-/-}$	*Cavin-1*$^{+/+}$	*Cavin-1*$^{-/-}$
Heart rate (beats/min)	398 ± 17 (n = 16)	458 ± 16* (n = 16)	389 ± 11 (n = 11)	454 ± 20* (n = 7)	349 ± 10† (n = 8)	428 ± 1*† (n = 6)
Flow rate (mL/min/g)	18.4 ± 0.9 (n = 23)	16.3 ± 0.9 (n = 23)	16.7 ± 1.6 (n = 11)	19.9 ± 1.1 (n = 8)	14.8 ± 0.5 (n = 8)	16.2 ± 0.4 (n = 6)
LV diastolic pressure (mmHg)	5.8 ± 0.4 (n = 15)	5.3 ± 0.8 (n = 13)	15 ± 7 (n = 11)	22 ± 3 (n = 8)	8 ± 2 (n = 8)	13 ± 2 (n = 6)
LV systolic pressure (mmHg)	106 ± 4 (n = 15)	95 ± 5 (n = 13)	132 ± 9 (n = 11)	128 ± 6 (n = 8)	117 ± 6 (n = 8)	107 ± 6* (n = 6)
LV developed pressure (mmHg)	100 ± 4 (n = 15)	90 ± 5 (n = 13)	117 ± 8 (n = 11)	107 ± 4 (n = 8)	109 ± 5 (n = 8)	93 ± 6 (n = 6)
$+dP/dt_{max}$ (mmHg/s)	3489 ± 494 (n = 15)	3913 ± 135 (n = 13)	4822 ± 213 (n = 11)	4778 ± 255 (n = 8)	4550 ± 317 (n = 8)	3925 ± 273 (n = 6)
$-dP/dt_{min}$ (mmHg/s)	−2236 ± 434 (n = 15)	−2606 ± 120 (n = 13)	−2843 ± 95 (n = 11)	−2939 ± 119 (n = 8)	−2708 ± 183 (n = 8)	−2440 ± 197 (n = 6)

Data were acquired from: 2 months hearts at a ventricular volume yielding an end-diastolic pressure of ~5 mmHg; and in 5–6 months hearts during peak volume-dependent pressure development (from data in Fig. 2). Values are mean ± SEM

*$P < 0.05$ vs. *cavin-1*$^{+/+}$; $^{\dagger}P < 0.05$ vs. untreated

cavin-1$^{-/-}$ hearts due to baseline vasodilatation (Fig. S5), while % debt repayment (which tended to increase with occlusion duration) was comparable in the two groups (Fig. S5). Treatment with L-NAME exerted greater effects on flow in *cavin-1*$^{-/-}$ vs. *cavin-1*$^{+/+}$ hearts, normalising baseline flow across groups and significantly reducing hyperaemia durations in *cavin-1*$^{-/-}$ hearts without impacting peak dilatation (Fig. 4b). Delineation of NOS-dependent and -independent flows (L-NAME-sensitive and -insensitive, respectively) confirms specific impacts of cavin-1 deletion on NOS-dependent function (Fig. 4a).

Masking of functional hyperaemia via NOS activity in hearts of *cavin-1*$^{-/-}$ mice

Noted above, functional hyperaemia was evident in *cavin-1*$^{+/+}$ hearts, with flow increasing linearly with ventricular pressure work (Fig. 4c). In contrast, flow remained stable across loads in *cavin-1*$^{-/-}$ hearts (slope of flow-pressure relation statistically indistinguishable from 0), at an elevated level equivalent to maximal flows achieved in *cavin-1*$^{+/+}$ hearts (Fig. 4c). Treatment with L-NAME did not eliminate functional hyperaemia in *cavin-1*$^{+/+}$ hearts, but induced a parallel shift to lower flows (Fig. 4c). In *cavin-1*$^{-/-}$ hearts L-NAME reduced basal flow and exposed a functional hyperaemia equivalent to that in *cavin-1*$^{+/+}$ hearts (Fig. 4c). The slopes of flow-LVDP relationships were comparable in *cavin-1*$^{+/+}$, *cavin-1*$^{+/+}$+ L-NAME and *cavin-1*$^{-/-}$ + L-NAME groups, revealing a consistent activity-dependent and NOS-independent hyperaemia of 5–8 mL/min/g per 100 mmHg ventricular pressure development. This hyperaemia may be blunted, in turn, by associated elevations in diastolic pressure (compression) at higher ventricular volumes: analysis of the relation between coronary flow and diastolic pressure in hearts treated with SNP (coronaries near maximally dilated) supports a 0.27 mL/min/g fall in coronary flow per 1 mmHg elevation in diastolic pressure (Fig. S4), similar to prior data for normoxic and post-ischaemic hearts [34]. Data collectively support a fixed contribution of NOS to basal coronary tone (exaggerated with cavin-1 deletion), while peak reactive hyperaemia and functional hyperaemia are largely NOS-independent.

Reduced ischaemic tolerance in hearts of *cavin-1*$^{-/-}$ mice

Outcomes from ischaemia were worsened in *cavin-1*$^{-/-}$ hearts (Fig. 5). Despite modest inhibition of early ischaemic contracture, post-ischaemic diastolic dysfunction was exaggerated (Fig. 5a; Fig. S6) and recoveries of pressure development and dP/dt_{max} and dP/dt_{min} impaired (Fig. 5b, c; Fig. S6). These effects appeared more pronounced in

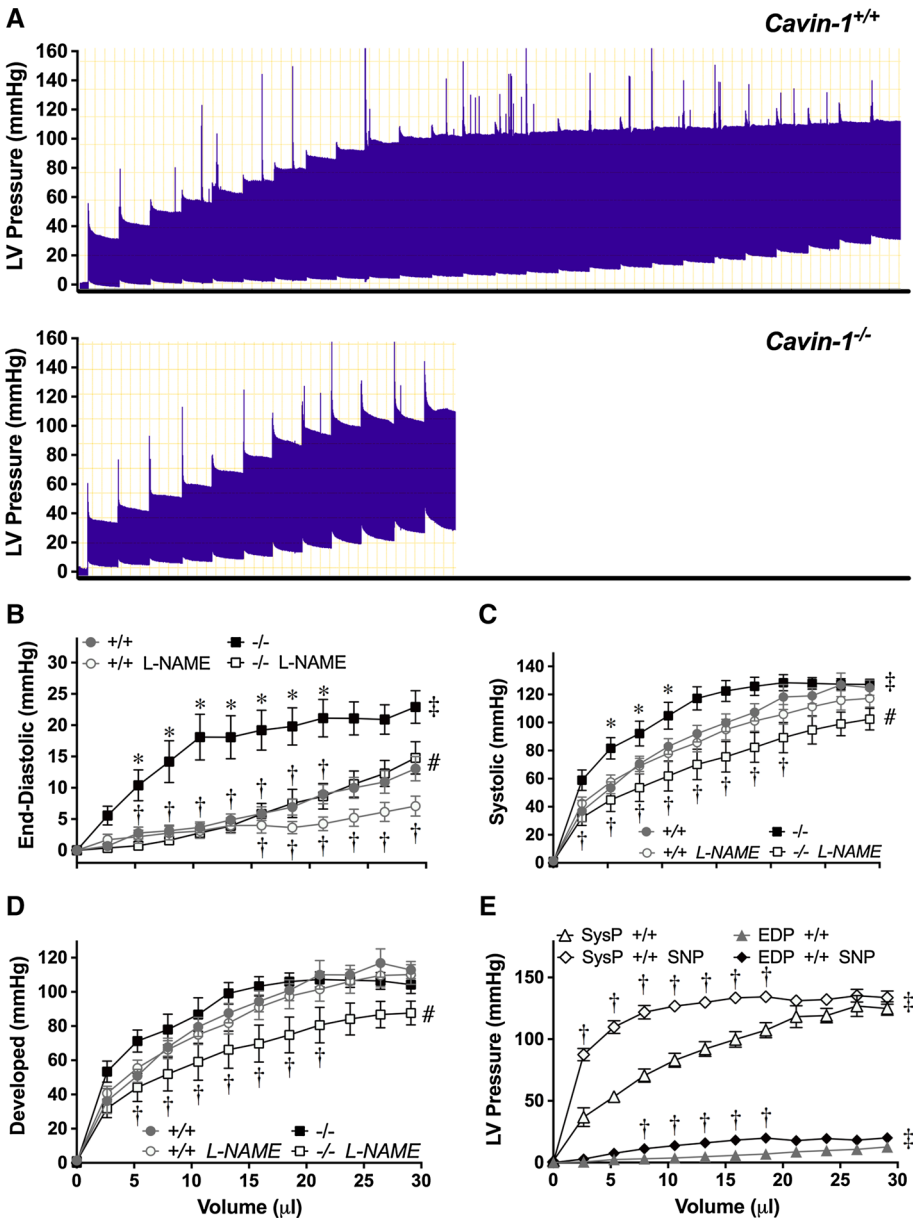

Fig. 3 Increased diastolic (passive) and systolic (active) pressures during ventricular stretch in hearts of *cavin-1*$^{-/-}$ mice. Left ventricular volume was incrementally increased and function assessed in untreated hearts (*cavin-1*$^{+/+}$, $n = 11$; *cavin-1*$^{-/-}$, $n = 9$), and L-NAME treated hearts (*cavin-1*$^{+/+}$, $n = 13$; *cavin-1*$^{-/-}$, $n = 7$). **a** Representative trace of left ventricular function in *cavin1*$^{+/+}$ (*upper*) and *cavin1*$^{-/-}$ (*lower*) hearts, and changes in; **b** end-diastolic pressure; **c** systolic pressure; **d** developed pressure. **e** Effects of 100 µM SNP on ventricular pressures in *cavin-1*$^{+/+}$ hearts (untreated, $n = 11$; SNP, $n = 6$). Data are mean ± SEM. $^{*}P < 0.05$ vs. *cavin-1*$^{+/+}$; $^{\dagger}P < 0.05$ vs. untreated; $^{\ddagger}P < 0.05$ vs. *cavin-1*$^{+/+}$ (AUC); $^{\#}P < 0.05$ vs. untreated (AUC)

male hearts (Fig. S6). Early functional rebound in the initial 2–5 min of reperfusion was largely absent in *cavin-1*$^{-/-}$ hearts, indicating exaggerated 'ischaemic' injury (though initial contracture was slightly reduced in *cavin-1*$^{-/-}$ hearts). Cell death/disruption was exaggerated in *cavin-1*$^{-/-}$ hearts, with significantly increased post-ischaemic LDH efflux (Fig. 5e; Fig. S6). Coronary reflow was also attenuated in *cavin-1*$^{-/-}$ hearts (Fig. 5d; Fig. S5), consistent with inhibitory effects of both elevated diastolic pressure (vascular compression; Fig. S4B) and reduced contractile function (metabolic demand) [34]. No differences in post-ischaemic phospho-activation of survival (AKT, ERK1/2) or stress kinases (JNK, p38-MAPK) were evident in *cavin-1*$^{-/-}$ vs. *cavin-1*$^{+/+}$ hearts (Fig. S7).

Impaired stretch-dependent signalling and exaggerated protein efflux in hearts of *cavin-1*$^{-/-}$ mice

Basal efflux of LDH was higher in *cavin-1*$^{-/-}$ vs. *cavin-1*$^{+/+}$ hearts (Figs. 5d, 6a), as was efflux of cardiac-specific cTnI (Fig. 6a), suggesting increased membrane fragility/permeability consistent with elevated serum creatine kinase observed in patients with cavin mutations [43]. To investigate further we assessed stretch-dependent protein efflux and signalling in hearts perfused at 1 or 3 mL/min, generating vascular pressures of 25–45 and 90–115 mmHg. At both low and high pressures, LDH efflux was greater in *cavin-1*$^{-/-}$ vs. *cavin-1*$^{+/+}$ hearts (Fig. 6a). Perfusion at elevated pressure

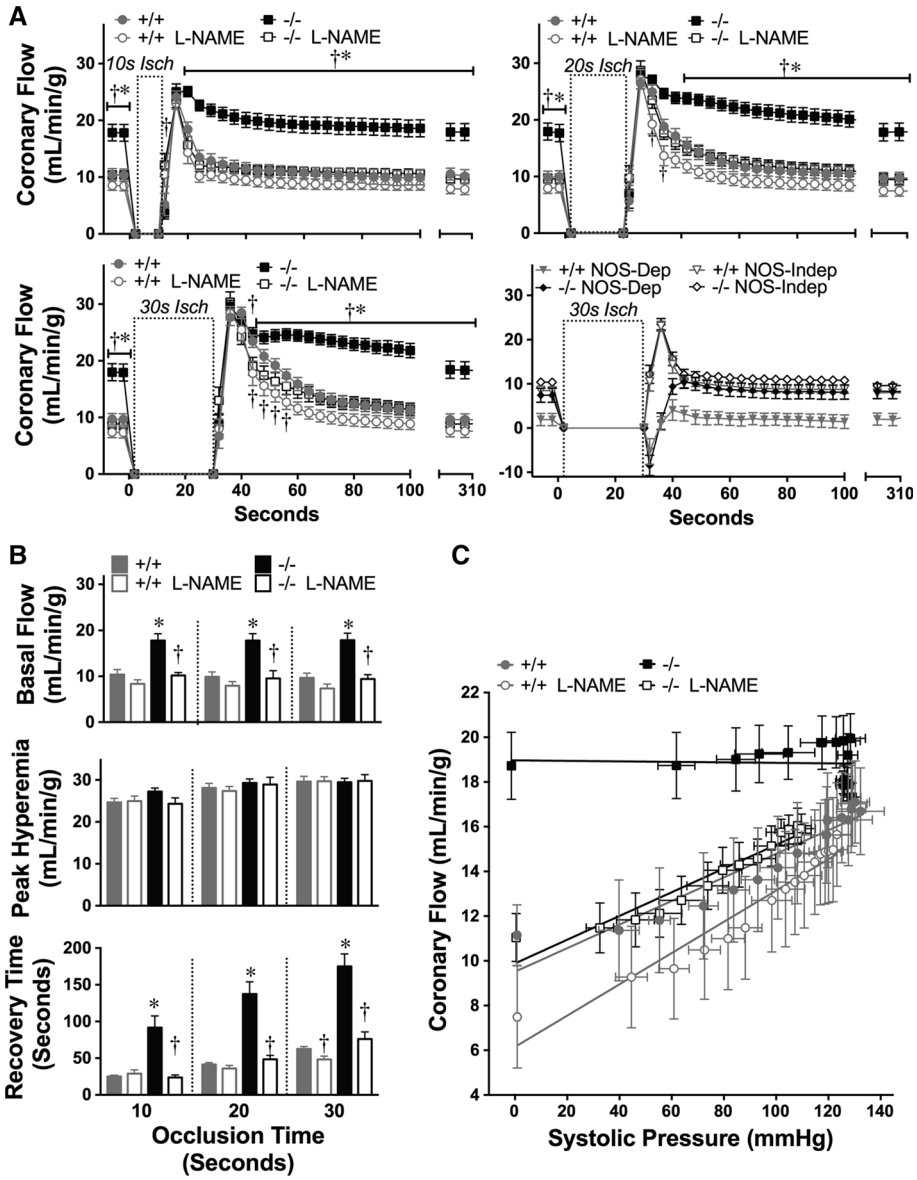

Fig. 4 Increased coronary flow and reactive hyperaemic duration, and masking of metabolic hyperaemia in hearts of *cavin-1*$^{-/-}$ mice. **a** Reactive hyperaemia after 10, 20 and 30 s occlusions in untreated *cavin-1*$^{+/+}$ ($n = 7$) and *cavin-1*$^{-/-}$ ($n = 8$) and 100 μM L-NAME treated *cavin-1*$^{+/+}$ ($n = 11$) and *cavin-1*$^{-/-}$ ($n = 7$) hearts. Both NOS-dependent (L-NAME-sensitive) and independent (L-NAME-insensitive) components are also shown. **b** Basal and peak reactive hyperaemic flows, and time for recovery of flow (by 90%) following peak hyperaemia. **c** Functional hyperaemia (coupling of flow to ventricular contractile function) in *cavin-1*$^{+/+}$ and *cavin-1*$^{-/-}$ hearts (±100 μM L-NAME). Data are mean ± SEM. *$P < 0.05$ vs. *cavin-1*$^{+/+}$; †$P < 0.05$ vs. untreated

also induced stretch-sensitive BNP and c-Fos, a response attenuated in *cavin-1*$^{-/-}$ hearts (Fig. 6a; Fig. S8). In contrast, ERK1/2 phospho-activation was similar in *cavin-1*$^{-/-}$ and $^{+/+}$ tissue (Fig. 6b; Fig. S7).

Injection of Evans blue to assess vascular permeability did not reveal differences in dye staining indicative of plasma membrane damage between *cavin-1*$^{+/+}$ and *cavin-1*$^{-/-}$ hearts. Microscopic inspection of cryosections revealed staining in a fraction of coronary vessels, co-localised with endothelial CD-31 (Fig. 6c). The ratio of stained vessels/total vessels was similar (0.34 ± 0.10 in *cavin-1*$^{+/+}$, $n = 5$ vs. 0.35 ± 0.06 in *cavin-1*$^{-/-}$, hearts, $n = 3$). Endothelial cells lining the ventricle were also stained, though we did not observe significant staining in the microvasculature (Fig. 6c). Some cardiomyocytes took up Evans blue, sometimes scattered as clusters of cells adjacent to blood vessels, however, this was not modified in *cavin-1*$^{-/-}$ hearts.

Discussion

Myocardial and coronary responses to both mechanical stretch and ischaemic insult are impaired in *cavin-1*$^{-/-}$ hearts, with normalisation of compliance, Frank–Starling behaviour and coronary function upon NOS inhibition implicating a dominant role for NOS over-activity in these phenotypic outcomes. However, cavin-1 deletion also led to NOS-independent positive chronotropy and negative inotropy. These alterations in function and stress-resistance are associated with (and may involve) impaired stretch-dependent signalling and exaggeration of membrane

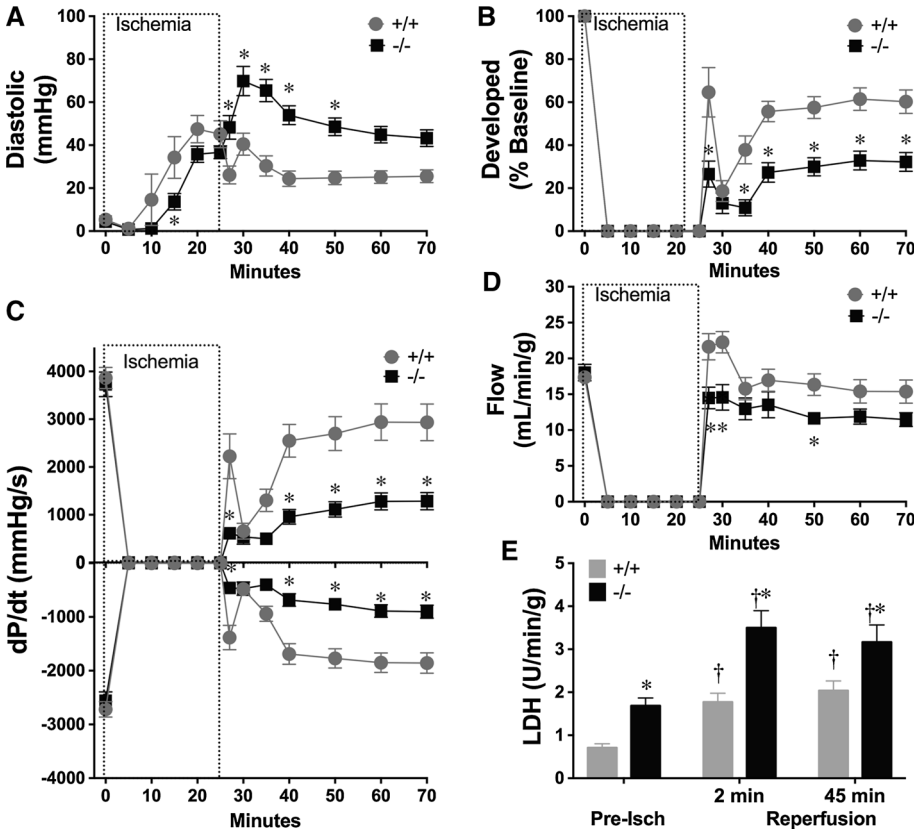

Fig. 5 Impaired ischaemic tolerance in hearts of *cavin-1*$^{-/-}$ mice. Data are shown for changes in: **a** left ventricular end-diastolic pressure; **b** developed pressure (% pre-ischaemia); **c** d*P*/dt_{max} and d*P*/dt_{min}, **d** coronary flow rate and **e** LDH efflux. Data are mean ± SEM (n = 20–21 for *cavin-1*$^{+/+}$; n = 21–22 for *cavin-1*$^{-/-}$). *$P < 0.05$ vs. *cavin-1*$^{+/+}$. Diastolic pressures from 15 min reperfusion in *cavin-1*$^{+/+}$ and 20 min in *cavin-1*$^{-/-}$ hearts differ from baseline ($P < 0.05$); coronary flow differs from baseline at 30 min in *cavin-1*$^{+/+}$ and 35, 50, 60, 70 min in *cavin-1*$^{-/-}$ hearts; developed pressures and d*P*/dt_{max} and d*P*/dt_{min} differs from baseline throughout reperfusion

fragility/permeability. Highlighting the importance of cavin-1 and associated proteins in governing chronotropic and inotropic function, and myocardial responses to mechanical load and ischaemia, these observations additionally reveal the potential for distinct outcomes with targeted or pathologic disruption of inter-related elements of the caveolar system. Changes in diastolic force also challenge the notion of NO-dependent maintenance of diastolic compliance [71].

Stretch-dependent myocardial function

A striking impact in *cavin-1*$^{-/-}$ hearts was a NOS-dependent increase in volume-dependent diastolic pressure (Fig. 3a). Insensitivity of the diastolic PVR to L-NAME across much of the volume range in *cavin-1*$^{+/+}$ hearts indicates endogenous NO normally only influences compliance at high loads in wild-types, and that NOS over-activity with cavin-1 deletion is detrimental (consistent with effects of SNP). Stretch-dependent systolic force was also cavin-1 dependent, involving NOS-dependent positive vs. NOS-independent negative inotropy (Fig. 3; Fig. S3). Distinct from loss of caveolin-1 or -3 [21, 107, 108, 114], or expression of a caveolin-3 mutant [67], there is little evidence of ventricular fibrosis/hypertrophy in the *cavin-1*$^{-/-}$ hearts studied, with contractility well maintained via NOS. Acute reversal with NOS inhibition confirms a functional rather than structural basis to reduced compliance and hypercontractility in *cavin-1*$^{-/-}$ hearts. These outcomes are also unrelated to increased beating rate in *cavin-1*$^{-/-}$ hearts (Table 2), as pacing was employed to normalise rates in these experiments. Moreover, distinct from contractile changes, the 60–65 beat/min difference in intrinsic rate was attenuated but not blocked by NOS inhibition (Table 2). Positive chronotropy is also reported with caveolin-1 knockout [20], though not caveolin-3 deletion.

Over-activity of NOS is congruent with increased vascular eNOS activity in *cavin-1*$^{-/-}$ mice [91, 92], and is likely secondary to suppression of caveolae and caveolins 1 and 3 [57, 94] (Figs. 1, 2), leading to dis-inhibition of eNOS [32, 65] (Fig. 7). The dominant myocardial isoform, eNOS is localised to the plasma membrane where it uniquely undergoes myristoylation and palmitoylation to drive inhibitory localisation to caveolae [33]. Depletion of caveolae thus over-activates eNOS, which is also the only isoform inhibited by cellular caveolin-1 [65] (an interaction promoted by caveolin-1 phosphorylation [17]). Caveolin-3 may similarly inhibit eNOS, though this is even less well defined [32, 33]. Whether these inhibitory effects occur via specific caveolin scaffold domains vs. other molecular sites or mechanisms also remains

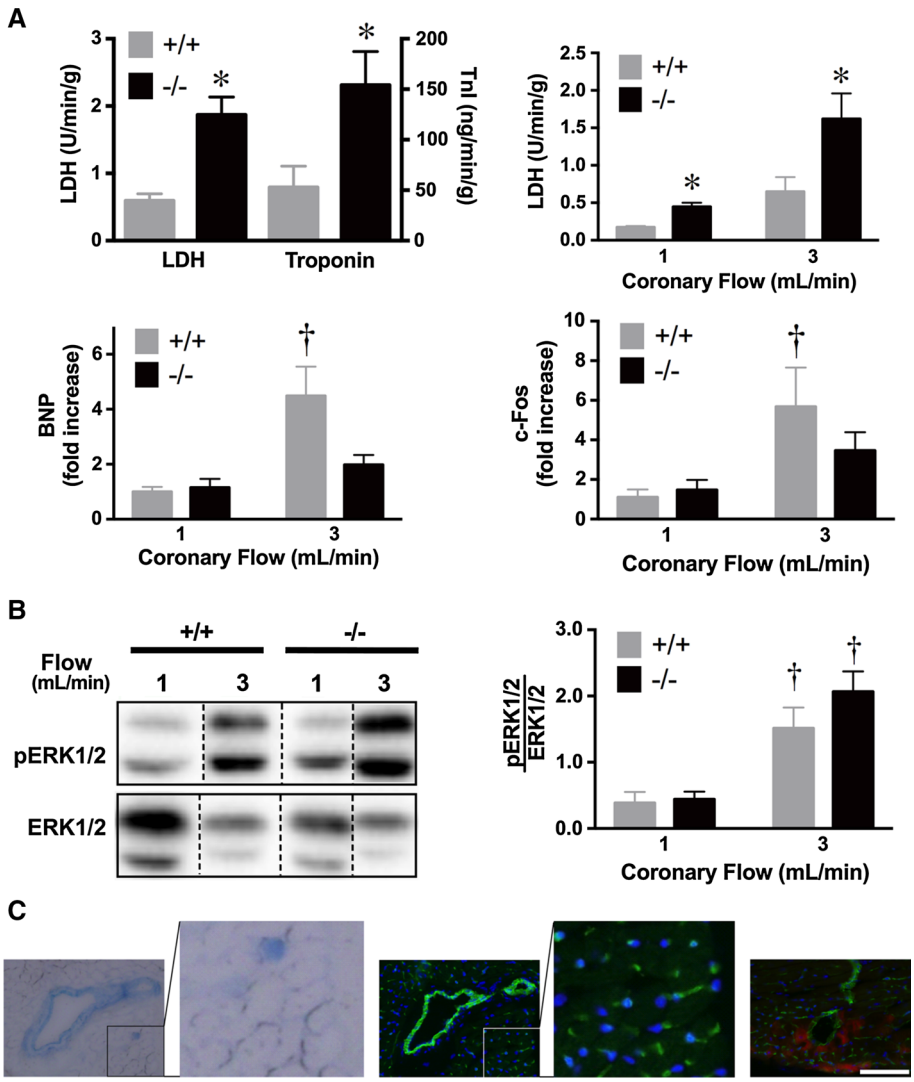

Fig. 6 Exaggerated basal and stretch-dependent protein efflux, and impaired stretch-dependent signalling in hearts of *cavin-1*$^{+/+}$ mice. **a** Efflux of LDH ($n = 12$/group) and cTnI ($n = 6$–7/group) in female hearts perfused at 80 mmHg; and perfusion pressure dependent LDH efflux, and BNP and c-Fos induction in male hearts ($n = 5$–7/group). **b** Perfusion pressure dependent changes in expression and phosphorylation of ERK1/2 in male hearts ($n = 3$–4/group). **c** *Left* Bright field image demonstrating Evans blue uptake into CD-31 positive cells (*middle*, *green*) of coronary vessels in a *cavin-1*$^{-/-}$ heart. Nuclei are stained with DAPI (*blue*). Evans blue staining was also detected in endothelial cells in *cavin-1*$^{+/+}$ hearts. Insets show no significant staining in endothelial cells/microvasculature between cardiomyocytes. *Right* Epi-fluorescence micrograph demonstrating Evans blue uptake into cardiomyocytes (*red*) adjacent to coronary vessels (*green*). *Scale bar* 100 µm. Data are mean ± SEM. *$P < 0.05$ vs. *cavin-1*$^{+/+}$; †$P < 0.05$ vs. 1 ml/min

debatable [22]. It is possible neuronal and inducible NOS could also contribute to L-NAME sensitive outcomes documented here, since caveolin-1 and caveolin-3 scaffold peptides appear to inhibit purified forms of all NOS isoforms in solution [36]. However, only eNOS activity is sensitive to cellular caveolin-1 [65]. Nonetheless, caveolin-1 depletion could boost iNOS levels, based on effects on iNOS degradation in other cells [31]; and despite primarily sarcoplasmic reticulum (SR) localisation of nNOS [110], there is biochemical (though not morphologic) evidence it co-localises with plasma membrane and caveolin-3 [25]. Importantly, excess NO may also be derived paracellularly from vascular endothelium: endothelial-derived NO has capacity to influence cardiomyocyte function [5], and cardiac effects of caveolin-1 deletion are reversed with endothelial specific re-expression [66]. Nonetheless, the phenotype in *cavin-1*$^{-/-}$ mice is not entirely compatible with *caveolin-1*$^{-/-}$ mice [108], suggesting unique influences of cavin-1.

The current findings are in partial agreement with recent analysis of female *cavin-1*$^{-/-}$ mice, published on completion of the present work [94]. Cardiac dysfunction in vivo in females studied by Taniguchi et al. is consistent with functional depression here (Table 1), an effect potentially more pronounced in females than males (Table S1). This may reflect evidence of more prominent NOS-independent negative inotropy in female *cavin-1*$^{-/-}$ myocardium (Fig. S3). On the other hand, body weight was reduced ~20% in *cavin-1*$^{-/-}$ vs. *cavin-1*$^{+/+}$ mice studied by Taniguchi et al., contrasting the current and prior studies [29, 52, 57]. A 15% fall in cardiac mass was also reported, despite 30–40% increases in ventricular wall thicknesses and myocyte size, together with significant fibrosis [94]. We also observe reduced heart mass normalised to body weight (with absolute weights similar for *cavin-1*$^{-/-}$ and *cavin-1*$^{+/+}$ hearts from 2 to 6 months), however, ventricular wall dimensions were unaltered with little evidence of fibrosis at 2 months (Table 1; Fig. 1).

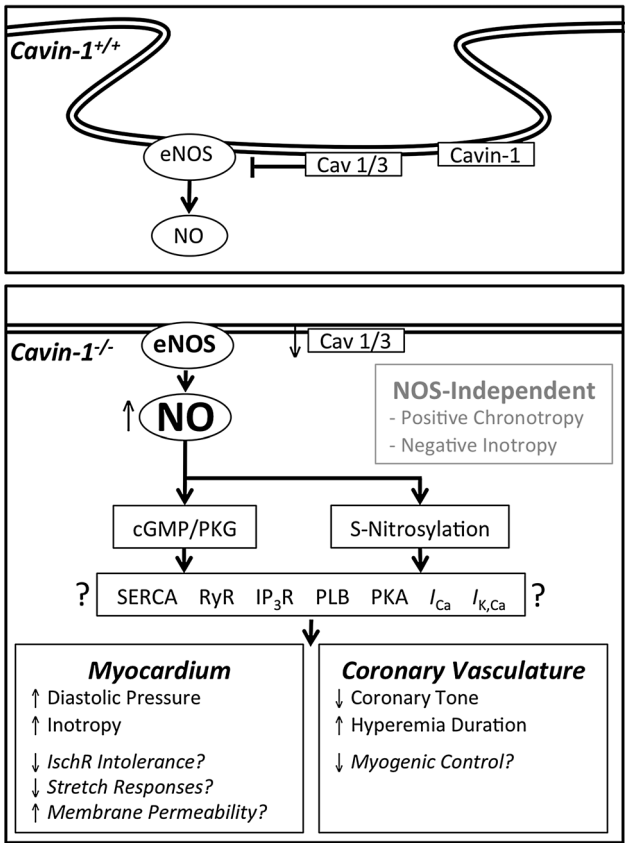

Fig. 7 Summary of cardiovascular impacts of cavin-1 deletion. Caveolin-1 and caveolin-3 (Cav1/3) co-associate with and are stabilised by cavin-1 in caveolae, where they inhibit localised endothelial nitric oxide synthase (eNOS). In *cavin-1*$^{-/-}$ hearts, Cav1/3 expression and localisation is disrupted, and caveolae do not form. These changes 'disinhibit' eNOS, promoting NO production and diastolic dysfunction, positive inotropy and coronary dilatation. Over-active NOS may also contribute to reduced tolerance to ischaemia–reperfusion (IschR), alterations in stretch signalling and membrane permeability/fragility, and impaired myogenic control. Potential NO effectors include cyclic guanosine monophosphate (cGMP)/protein kinase G (PKG) dependent signalling and/or S-nitrosylation, known to modulate the sarcoplasmic reticulum Ca^{2+}-ATPase (SERCA), ryanodine receptor (RyR), inositol triphosphate receptor (IP3R), phospholamban (PLB), and plasma membrane Ca^{2+} (I_{Ca}) and Ca^{2+}-activated K^+ ($I_{K,Ca}$) channels. NOS-independent effects of cavin-1 deletion are also shown

Reported electrocardiographic abnormalities, including suppression of R-waves and broadening of the QRS complex [94], were also not evident here. However, we detect a significantly elevated (NOS-independent) intrinsic beating rate (Table 2), which is consistent with depression of caveolin-3 protein in *cavin-1*$^{-/-}$ hearts—caveolin-3 has been shown to slow the heart while increasing expression of voltage-gated K^+ and Na^+ channels and connexin-43 [85]. Reasons for these mixed outcomes are unclear, though it is possible fibrosis/hypertrophy evolves with further age in *cavin-1*$^{-/-}$ animals. Murine genetic background is also relevant, both to normoxic function and cardiac stress responses [4]: mice studied here are C57Bl/6/CD-1 hybrids while Taniguchi et al. report specifically on female *cavin-1*$^{-/-}$ mice on a C57Bl/6 background [94]. Importantly, shifts in peripheral/pulmonary vascular control and pressures [91, 92], together with autonomic regulation, will influence cardiac function in situ, complicating interpretation. In contrast, ex vivo analysis unmasks intrinsic changes in myocardial contractile properties: our data identify a functional rather than structural phenotype in young *cavin-1*$^{-/-}$ hearts, characterised by NOS-dependent shifts in stretch-dependent contractile force, and NOS-independent chronotropy and negative inotropy.

Diastolic compliance

A NOS-dependent elevation in the diastolic PVR with cavin-1 deletion contrasts early in vivo studies supporting downward shifts with NO donors, initially attributed to ventricular unloading and biventricular interaction secondary to venodilation [11]. Although some subsequent investigations report reduced diastolic stiffness with drugs increasing NO levels [53, 71, 72], others find physiologic NO levels exert no effects [54, 75] or increase diastolic pressure [60]. Consistent with our findings, Wunderlich et al. document a NOS-dependent elevation in diastolic pressure in hearts lacking caveolin-1 [108]. These findings collectively support a stimulatory effect of NOS over-activity on stretch-dependent diastolic force in hearts deficient in either cavin-1 or caveolin-1. These findings contrast the notion that elevated NO improves diastolic function while reductions underlie diastolic dysfunction or stiffening [71]. Mechanistically, NOS-dependent diastolic stiffness may involve NO-dependent modulation of stretch-dependent SR Ca^{2+} release [99], and ryanodine receptor (RyR) function and Ca^{2+} leak [39, 109] (Fig. 7). Endogenous NO from eNOS or nNOS can also inhibit SR Ca^{2+}-pump activity to slow relaxation and potentially increase intracellular [Ca^{2+}] [110, 116]. Metabolites of NO may also be relevant: peroxynitrite formation with NO overproduction may contribute to dysfunction as peroxynitrite increases diastolic pressure [41]; and NO uptake into erythrocytes results in rapid co-oxidation with oxyhaemoglobin/haemoglobin to form more stable and bioactive *S*-nitrosothiols [78] which could additionally influence function. The release of NO from erythrocytes, coupled with generation via NOS, results in greater NO availability for reactions with reactive oxygen species in vivo. Such processes may contribute to differing effects of chronic endogenous NO production (the present study and [108]) and acutely applied NO donors.

NOS-dependent inotropy

A NOS-dependent inotropy in *cavin-1*$^{-/-}$ hearts (Fig. 3b) is consistent with effects of SNP in *cavin-1*$^{+/+}$ hearts (Fig. 3d). Both endogenous and exogenous NO can increase contractility in isolated cells/tissue [3, 54, 55], and intact heart and in vivo studies support NOS [74] and specific eNOS dependence [5, 16, 38] of cardiac contractility. Distinct functional outcomes may arise via spatial confinement of NOS signalling, with caveolar eNOS modulating co-localised L-type Ca^{2+} channels and β-adrenergic receptors, and SR nNOS targeting RyR function and SR Ca^{2+} handling [5]. Furthermore, local and peripheral vascular eNOS activities [5, 79, 101], together with circulating eNOS [40, 64], may influence myocardial function or phenotype. Exogenous NO may additionally exert functional effects via generation of *S*-nitrosothiols or nitrite within the circulation [78, 79]. The molecular mechanisms underlying NOS-dependent inotropy evident in ex vivo myocardium here await clarification, however, NO: activates L-type Ca^{2+} channels and sensitises Ca^{2+}-dependent SR Ca^{2+} release via S-nitrosylation [15, 65]; enhances stretch-dependent SR Ca^{2+} release, contributing to Frank–Starling responses [99]; and may also promote phospholamban phosphorylation [103] (Fig. 7).

NOS-independent negative inotropy

The basis of NOS-independent negative inotropy (Fig. 3; Fig. S3) in *cavin-1*$^{-/-}$ hearts (prominent in females) warrants further study, though is consistent with depressed in vivo function in females, and contractile effects of caveolar disruption with methyl-β-cyclodextrin [14, 88] or caveolin-1 deficiency [21, 108, 114] (though the latter likely reflects NOS effects). Caveolar disruption with cavin-1 deletion is predicted to impair inotropy given caveolar dependencies of Ca^{2+} channels [37] and excitation–contraction coupling [14, 90]. Positive chronotropy and tendency to arrhythmicity in *cavin-1*$^{-/-}$ hearts are consistent with disturbed channel function. Disruption of caveolin-3 may also reduce contractility, if interacting with cardiac RyRs as in skeletal muscle [105]. While caveolin-3 deletion does not appear to alter intrinsic myocardial contractility (distinct from caveolar disruption) [88], stretch-dependent function has yet to be adequately assessed in this model. However, contractility is ultimately compromised with progressive hypertrophy in these mice [107]. In contrast, mutant caveolin-3 increases contractility and eNOS activity in association with hypertrophy [67]. Deletion of cavin-1 also impairs contraction in smooth muscle [52], and broad differences in muscle function could arise from altered expression of proteins governing contraction, given transcriptional influences of cavin-1 [50]. Finally, reduced contractility in the presence of NOS inhibition in *cavin-1*$^{-/-}$ vs. *cavin-1*$^{+/+}$ hearts may additionally reflect adaptation to chronically elevated (positive inotropic) NO.

Coronary vasoregulation

Genetic deletion of cavin-1, and NOS inhibition, specifically modified baseline flow and reactive hyperaemia durations, while peak hyperaemic flows were unaltered and metabolic hyperaemia was effectively masked (Fig. 4). These findings are congruent with reduced vascular tone in mesenteric arteries from *cavin-1*$^{-/-}$ mice [91], together with increased coronary flow [20] and augmented NO-dependent aortic dilatation vs. impaired constriction with caveolin-1 knockout [80]. These outcomes are also consistent with NOS-dependence of basal tone in mammalian coronaries [68, 89, 97], NOS-independence of peak hyperaemic flows vs. NOS-dependence of reactive hyperaemia duration [28, 76, 113], and NOS-independence of vasodilatation during increases in MVO_2 [30, 96]. Although our data confirm involvement of NO in prolonging hyperaemia [28, 76, 113], this seems unlikely to involve flow- or shear-dependent NOS activation, since the latter is caveola dependent [82] and inhibited on caveolin-1 deletion [2, 112]. Evidence of impaired coronary myogenic control in *cavin-1*$^{-/-}$ hearts (Fig. S4A) is also consistent with impaired control in mesenteric vessels following cavin-1 [91] or caveolin-1 deletion [2], and evidence NO impairs coronary autoregulation [97]. Interestingly, differences in baseline coronary flow between *cavin-1*$^{-/-}$ and $^{+/+}$ hearts are limited by NOS-independent functional hyperaemia. Ventricular pressure work induces a functional (metabolic) hyperaemia [81], evident here in *cavin-1*$^{+/+}$ hearts (Fig. 4c) yet masked by excess NOS-dependent dilation in *cavin-1*$^{-/-}$ hearts. Clearly depicted in Fig. 4c, NOS-independent functional hyperaemia progressively reduces differences in basal flow in *cavin-1*$^{-/-}$ vs. $^{+/+}$ hearts as pressure work increases. Inhibition of NOS reduces basal flow and reveals comparable hyperaemia in knockout hearts.

Myocardial ischaemic tolerance

The caveolar system appears important to ischaemic tolerance and cardioprotection [47, 69, 84, 88, 95]. In agreement with such roles, *cavin-1*$^{-/-}$ hearts exhibited worsened contractile dysfunction and cell damage following ischaemia (Fig. 5). Ischaemic intolerance may involve suppression of caveolins and caveolae (Figs. 1, 2), critical to myocardial stress responses [84, 88, 111]. Indeed, ischaemic intolerance is common to caveolin-3 knockout, and both caveolin-3 and caveolin-1 are repressed with cavin-1 deletion (Fig. 2) [57, 94]. Nonetheless, distinct

outcomes are evident in *cavin-1*$^{-/-}$ hearts. Caveolin-3 knockout fails to alter infarction [47] or worsens cell death without altering contractile dysfunction [88]. Moreover, although caveolin-3 modifies AKT phosphorylation [69, 95], and deletion of caveolin-3 or caveolin-1 triggers ERK1/2 hyper-activation [21, 107], post-ischaemic phosphorylation of these kinases (and injurious p38 MAPK and JNK) was unaltered in *cavin-1*$^{-/-}$ hearts (Fig. S7). Effects of caveolin-1 ablation on ischaemic tolerance are less clear, with no shift in infarction/cell death and either unaltered [26] or worsened [51, 69] contractile outcomes.

While ischaemic intolerance in *cavin-1*$^{-/-}$ hearts is not associated with shifts in post-ischaemic kinase signalling, altered membrane fragility and stretch responses and exaggerated NOS activity are likely to contribute (though are not tested here). Opposing effects of NOS/NO on ischaemic tolerance have been reported; with some studies supporting benefit via low physiologic NO levels vs. injury and dysfunction with excess NO [87]. Differing effects of NO donors on ischaemic outcomes in pre-clinical animal models vs. humans are also apparent, posing a challenge in development of potential NO-based cardioprotection [8]. The effects of NO and NOS activity on ischaemic tolerance may involve shifts in both injurious nitrosylation/nitrosative stress and protective PKG-dependent signalling, and effects of both native NO and circulating metabolites including nitrite and *S*-nitrosothiols [78, 79]. The ischaemic intolerance in *cavin-1*$^{-/-}$ hearts exhibiting over-active NOS is consistent with exaggerated injury via NOS activation/expression [48, 104] vs. protection via NOS inhibition [23, 27, 63, 86, 102, 104, 106]. Nonetheless, other studies suggest either no effect of NOS activity on ischaemic injury or metabolism [61, 73, 74], NOS-dependent induction of an early low-energy hibernating state [45], or conversely NOS-dependent injury [44, 48, 104]. These differing outcomes again reflect in part distinct effects of NOS isoforms and cellular NOS pools: ischaemic tolerance is enhanced via cardiac [12, 24] and circulating (erythrocyte) eNOS activities [40, 64], together with nitrite generated via peripheral vascular eNOS [79]; while myocardial iNOS promotes cell death [48, 104] and dysfunction [44]; and nNOS worsens ischaemic tolerance while paradoxically participating in downstream signalling underlying ischaemic preconditioning [6, 59]. It is also relevant that myocardial NO generation during ischaemia may arise via NOS-independent pathways [62], complicating interpretation of the effects of NOS modulation in ischaemia–reperfusion. Though not conclusive, and awaiting confirmation, the ischaemic intolerance in isolated myocardium from *cavin-1*$^{-/-}$ mice appears most consistent with dis-inhibition of protective (and caveolar/caveolin sensitive) eNOS [12, 24, 40, 64, 79, 115], rather than increased activities of injurious iNOS or nNOS.

Interestingly, despite evidence of NOS over-activity, post-ischaemic reflow was moderately reduced in *cavin-1*$^{-/-}$ vs. $^{+/+}$ hearts. This is consistent with limited NOS involvement in post-ischaemic hyperaemia (Fig. 4) [28, 76, 113]. The modest (~25%) difference in reflow does not explain ~twofold greater contractile dysfunction and cell death in *cavin-1*$^{-/-}$ hearts. Indeed, reductions in NO-dependent flow do not worsen post-ischaemic injury [104, 106]. Reduced reflow is consistent with differing diastolic compression and metabolic demand [34]: ~20 mmHg higher diastolic contracture is predicted to limit post-ischaemic flow by ~5 mL/min/g in *cavin-1*$^{-/-}$ hearts, based on effects documented here (Fig. S4B) and previously [34]; while reduced metabolic demand in *cavin-1*$^{-/-}$ hearts generating ~35% of baseline function (vs. 60% in *cavin-1*$^{+/+}$ hearts) will further limit flow (Fig. 4).

Membrane integrity and cellular stretch responses

The caveolar system plays an overarching role in cellular responses to stretch, and protection against mechanical perturbation [70]. Caveolae provide a membrane reserve or mechanical buffer to limit damage during stretch, and deformation may trigger intracellular changes via cavin-1 release into the cytoplasm [18, 70]. Cavin-1 [117], together with caveolin-1 [10] and -3 [13], are also implicated in membrane repair and stretch-dependent signalling/mechanotransduction [49]. Global deletion of cavin-1 not only modified passive and active forces during myocardial stretch (Fig. 3), but inhibited stretch-dependent BNP and c-Fos induction, while ERK1/2 activation was unaltered (Fig. 6). The latter contrasts impaired ERK2 activation in cardiomyocytes lacking caveolin-3 [49], though is consistent with lack of effect of caveolin-3 knockdown on ERK2 activation in skeletal myotubes [9]. Lack of effect of cavin-1 deletion on kinase signalling (with stretch or ischaemia) localises the cavin-1-dependence of stretch signalling downstream of kinase activation processes.

Exaggerated basal and stretch-dependent efflux of cardiac proteins is consistent with reported effects of cavin-1 or caveolin-1 deletion on membrane fragility during stretch, shear stress and cell swelling [9, 58]. It remains to be elucidated whether NOS over-activation contributes to altered stretch-dependent signalling and membrane fragility in hearts lacking cavin-1. Nonetheless, these changes are likely to contribute to shifts in the stretch-dependence of mechanical function, and to ischaemic intolerance given fundamental roles of swelling and membrane rupture in post-ischaemic injury.

Concluding remarks

The current analyses reveal roles for cavin-1 and related proteins in governing myocardial contractile function and compliance, coronary and cardiac responses to mechanical and ischaemic stressors, and membrane permeability/fragility. Over-activity of NOS appears to underlie reversible elevations in stretch-dependent passive and active ventricular forces, baseline coronary flow and hyperaemia duration, while NOS-independent positive chronotropy and negative inotropy also arise in *cavin-1*$^{-/-}$ hearts. The NOS isoforms involved in the former phenotypic changes, their cellular and sub-cellular locations, and effector mechanisms downstream of NO overproduction (e.g. PKG- or nitrosylation-dependent shifts in sarcolemmal or SR Ca^{2+} handling) await analysis (Fig. 7). Importantly, cavin-1 deletion also inhibits stretch-dependent cardiac signalling and exaggerates membrane permeability/fragility, changes likely to impact myocardial function and ischaemic tolerance. While the molecular bases of these effects require further investigation, the present findings collectively highlight the broad importance (and potential utility) of cavin-1 and associated proteins in governing load-dependent cardiovascular phenotypes, membrane function, and myocardial stress-resistance.

Acknowledgements The authors acknowledge the excellent technical assistance of Sam Man Lee and statistical advice of Risto Bloigu, and use of the Australian Microscopy and Microanalysis Research Facility at the Center for Microscopy and Microanalysis at The University of Queensland. Fluorescence microscopy was performed at the Australian Cancer Research Foundation (ACRF)/Institute for Molecular Bioscience (IMB) Dynamic Imaging Facility for Cancer Biology.

Compliance with ethical standards

Conflict of interest The authors declare that they have no conflict of interest.

Sources of funding This research was supported by grants and a fellowship from the National Health and Medical Research Council of Australia to RGP (Grant Numbers APP1037320, APP1058565 and APP569542) and a grant to WGT (APP1085996). MK was recipient of a fellowship from the Academy of Finland (Decision 266263).

Ethical standards All animal experiments were approved by the University of Queensland Ethics Committee (SBMS/044/15/AIBN/IMB) and were performed in accordance with the ethical standards laid down in the 1964 Declaration of Helsinki and its later amendments.

References

1. Aboulaich N, Chui PC, Asara JM, Flier JS, Maratos-Flier E (2011) Polymerase I and transcript release factor regulates lipolysis via a phosphorylation-dependent mechanism. Diabetes 60:757–765. doi:10.2337/db10-0744
2. Albinsson S, Shakirova Y, Rippe A, Baumgarten M, Rosengren BI, Rippe C, Hallmann R, Hellstrand P, Rippe B, Swärd K (2007) Arterial remodeling and plasma volume expansion in caveolin-1-deficient mice. Am J Physiol Regul Integr Comp Physiol 293:R1222–R1231. doi:10.1152/ajpregu.00092.2007
3. Angelone T, Quintieri AM, Pasqua T, Filice E, Cantafio P, Scavello F, Rocca C, Mahata SK, Gattuso A, Cerra MC (2015) The NO stimulator, Catestatin, improves the Frank–Starling response in normotensive and hypertensive rat hearts. Nitric Oxide 50:10–19. doi:10.1016/j.niox.2015.07.004
4. Barnabei MS, Palpant NJ, Metzger JM (2010) Influence of genetic background on ex vivo and in vivo cardiac function in several commonly used inbred mouse strains. Physiol Genomics 42A:103–113. doi:10.1152/physiolgenomics.00071.2010
5. Barouch LA, Harrison RW, Skaf MW, Rosas GO, Cappola TP, Kobeissi ZA, Hobai IA, Lemmon CA, Burnett AL, O'Rourke B, Rodriguez ER, Huang PL, Lima JA, Berkowitz DE, Hare JM (2002) Nitric oxide regulates the heart by spatial confinement of nitric oxide synthase isoforms. Nature 416:337–339. doi:10.1038/416005a
6. Barua A, Standen NB, Galiñanes M (2010) Dual role of nNOS in ischemic injury and preconditioning. BMC Physiol 10:15. doi:10.1186/1472-6793-10-15
7. Bastiani M, Liu L, Hill MM, Jedrychowski MP, Nixon SJ, Lo HP, Abankwa D, Luetterforst R, Fernandez-Rojo M, Breen MR, Gygi SP, Vinten J, Walser PJ, North KN, Hancock JF, Pilch PF, Parton RG (2009) MURC/Cavin-4 and cavin family members form tissue-specific caveolar complexes. J Cell Biol 185:1259–1273. doi:10.1083/jcb.200903053
8. Bice JS, Jones BR, Chamberlain GR, Baxter GF (2016) Nitric oxide treatments as adjuncts to reperfusion in acute myocardial infarction: a systematic review of experimental and clinical studies. Basic Res Cardiol 111:23. doi:10.1007/s00395-016-0540-y
9. Bellott AC, Patel KC (1985) Burkholder TJ (2005) Reduction of caveolin-3 expression does not inhibit stretch-induced phosphorylation of ERK2 in skeletal muscle myotubes. J Appl Physiol 2005(98):1554–1561. doi:10.1152/japplphysiol.01070.2004
10. Bernatchez PN, Sharma A, Kodaman P, Sessa WC (2009) Myoferlin is critical for endocytosis in endothelial cells. Am J Physiol Cell Physiol 297:C484–C492. doi:10.1152/ajpcell.00498.2008
11. Brodie BR, Grossman W, Mann T, McLaurin LP (1977) Effects of sodium nitroprusside on left ventricular diastolic pressure–volume relations. J Clin Invest 59:59–68. doi:10.1172/JCI108622
12. Brunner F, Maier R, Andrew P, Wölkart G, Zechner R, Mayer B (2003) Attenuation of myocardial ischemia/reperfusion injury in mice with myocyte-specific overexpression of endothelial nitric oxide synthase. Cardiovasc Res 57:55–62. doi:10.1016/S0008-6363(02)00649-1
13. Cai C, Weisleder N, Ko JK, Komazaki S, Sunada Y, Nishi M, Takeshima H, Ma J (2009) Membrane repair defects in muscular dystrophy are linked to altered interaction between MG53, caveolin-3, and dysferlin. J Biol Chem 284:15894–15902. doi:10.1074/jbc.M109.009589
14. Calaghan S, White E (2006) Caveolae modulate excitation-contraction coupling and beta2-adrenergic signalling in adult rat ventricular myocytes. Cardiovasc Res 69:816–824. doi:10.1016/j.cardiores.2005.10.006
15. Campbell DL, Stamler JS, Strauss HC (1996) Redox modulation of L-type calcium channels in ferret ventricular myocytes. Dual mechanism regulation by nitric oxide and S-nitrosothiols. J Gen Physiol 108:277–293. doi:10.1085/jgp.108.4.277
16. Champion HC, Georgakopoulos D, Takimoto E, Isoda T, Wang Y, Kass DA (2004) Modulation of in vivo cardiac function by

myocyte-specific nitric oxide synthase-3. Circ Res 94:657–663. doi:10.1161/01.RES.0000119323.79644.20
17. Chen Z, Bakhshi FR, Shajahan AN, Sharma T, Mao M, Trane A, Bernatchez P, van Nieuw Amerongen GP, Bonini MG, Skidgel RA, Malik AB, Minshall RD (2012) Nitric oxide-dependent Src activation and resultant caveolin-1 phosphorylation promote eNOS/caveolin-1 binding and eNOS inhibition. Mol Biol Cell 23:1388–1398. doi:10.1091/mbc.E11-09-0811
18. Cheng JP, Mendoza-Topaz C, Howard G, Chadwick J, Shvets E, Cowburn AS, Dunmore BJ, Crosby A, Morrell NW, Nichols BJ (2015) Caveolae protect endothelial cells from membrane rupture during increased cardiac output. J Cell Biol 211:53–61. doi:10.1083/jcb.201504042
19. Chiu HS, York JP, Wilkinson L, Zhang P, Little MH, Pennisi DJ (2012) Production of a mouse line with a conditional Crim1 mutant allele. Genesis 50(9):711–716. doi:10.1002/dvg.22032
20. Chow AK, Daniel EE, Schulz R (2010) Cardiac function is not significantly diminished in hearts isolated from young caveolin-1 knockout mice. Am J Physiol Heart Circ Physiol 299(4):H1183–H1189. doi:10.1152/ajpheart.01195.2009
21. Cohen AW, Park DS, Woodman SE, Williams TM, Chandra M, Shirani J, Pereira de Souza A, Kitsis RN, Russell RG, Weiss LM, Tang B, Jelicks LA, Factor SM, Shtutin V, Tanowitz HB, Lisanti MP (2003) Caveolin-1 null mice develop cardiac hypertrophy with hyperactivation of p42/44 MAP kinase in cardiac fibroblasts. Am J Physiol Cell Physiol 284:C457–C474. doi:10.1152/ajpcell.00380.2002
22. Collins BM, Davis MJ, Hancock JF, Parton RG (2012) Structure-based reassessment of the caveolin signaling model: do caveolae regulate signaling through caveolin-protein interactions? Dev Cell 23:11–20. doi:10.1016/j.devcel.2012.06.012
23. Csonka C, Szilvássy Z, Fülöp F, Páli T, Blasig IE, Tosaki A, Schulz R, Ferdinandy P (1999) Classic preconditioning decreases the harmful accumulation of nitric oxide during ischemia and reperfusion in rat hearts. Circulation 100:2260–2266. doi:10.1161/01.CIR.100.22.2260
24. Cuong DV, Kim N, Youm JB, Joo H, Warda M, Lee JW, Park WS, Kim T, Kang S, Kim H, Han J (2006) Nitric oxide-cGMP-protein kinase G signaling pathway induces anoxic preconditioning through activation of ATP-sensitive K^+ channels in rat hearts. Am J Physiol Heart Circ Physiol 290:H1808–H1817. doi:10.1152/ajpheart.00772.2005
25. Damy T, Ratajczak P, Shah AM, Camors E, Marty I, Hasenfuss G, Marotte F, Samuel JL, Heymes C (2004) Increased neuronal nitric oxide synthase-derived NO production in the failing human heart. Lancet 363:1365–1367. doi:10.1016/S0140-6736(04)16048-0
26. Das M, Das S, Lekli I, Das DKJ (2012) Caveolin induces cardioprotection through epigenetic regulation. Cell Mol Med 16:888–895. doi:10.1111/j.1582-4934.2011.01372.x
27. Depre C, Vanoverschelde JL, Goudemant JF, Mottet I, Hue L (1995) Protection against ischemic injury by nonvasoactive concentrations of nitric oxide synthase inhibitors in the perfused rabbit heart. Circulation 92:1911–1918. doi:10.1161/01.CIR.92.7.1911
28. Dick GM, Bratz IN, Borbouse L, Payne GA, Dincer UD, Knudson JD, Rogers PA, Tune JD (2008) Voltage-dependent K^+ channels regulate the duration of reactive hyperemia in the canine coronary circulation. Am J Physiol Heart Circ Physiol 294:H2371–H2381. doi:10.1152/ajpheart.01279.2007
29. Ding SY, Lee MJ, Summer R, Liu L, Fried SK, Pilch PF (2014) Pleiotropic effects of cavin-1 deficiency on lipid metabolism. J Biol Chem 289:8473–8483. doi:10.1074/jbc.M113.546242
30. Duncker DJ, Stubenitsky R, Tonino PA, Verdouw PD (2000) Nitric oxide contributes to the regulation of vasomotor tone but does not modulate O_2-consumption in exercising swine. Cardiovasc Res 47:738–748. doi:10.1016/S0008-6363(00)00143-7
31. Felley-Bosco E, Bender FC, Courjault-Gautier F, Bron C, Quest AF (2000) Caveolin-1 down-regulates inducible nitric oxide synthase via the proteasome pathway in human colon carcinoma cells. Proc Natl Acad Sci USA 97:14334–14339. doi:10.1073/pnas.250406797
32. Feron O, Belhassen L, Kobzik L, Smith TW, Kelly RA, Michel T (1996) Endothelial nitric oxide synthase targeting to caveolae. Specific interactions with caveolin isoforms in cardiac myocytes and endothelial cells. J Biol Chem 271:22810–22814. doi:10.1074/jbc.271.37.22810
33. Feron O, Dessy C, Opel DJ, Arstall MA, Kelly RA, Michel T (1998) Modulation of the endothelial nitric-oxide synthase-caveolin interaction in cardiac myocytes. Implications for the autonomic regulation of heart rate. J Biol Chem 273:30249–30254. doi:10.1074/jbc.273.46.30249
34. Flood AJ, Willems L, Headrick JP (2002) Coronary function and adenosine receptor-mediated responses in ischemic-reperfused mouse heart. Cardiovasc Res 55:161–170. doi:10.1016/S0008-6363(02)00329-2
35. Gambin Y, Ariotti N, McMahon KA, Bastiani M, Sierecki E, Kovtun O, Polinkovsky ME, Magenau A, Jung W, Okano S, Zhou Y, Leneva N, Mureev S, Johnston W, Gaus K, Hancock JF, Collins BM, Alexandrov K, Parton RG (2013) Single-molecule analysis reveals self assembly and nanoscale segregation of two distinct cavin subcomplexes on caveolae. eLife 3:e01434. doi:10.7554/eLife.01434
36. García-Cardeña G, Martasek P, Masters BS, Skidd PM, Couet J, Li S, Lisanti MP, Sessa WC (1997) Dissecting the interaction between nitric oxide synthase (NOS) and caveolin. Functional significance of the NOS caveolin binding domain in vivo. J Biol Chem 272:25437–25440. doi:10.1074/jbc.272.41.25437
37. Glukhov AV, Balycheva M, Sanchez-Alonso JL, Ilkan Z, Alvarez-Laviada A, Bhogal N, Diakonov I, Schobesberger S, Sikkel MB, Bhargava A, Faggian G, Punjabi PP, Houser SR, Gorelik J (2015) Direct evidence for microdomain-specific localization and remodeling of functional l-type calcium channels in rat and human atrial myocytes. Circulation 132:2372–2384. doi:10.1161/CIRCULATIONAHA.115.018131
38. Gödecke A, Heinicke T, Kamkin A, Kiseleva I, Strasser RH, Decking UK, Stumpe T, Isenberg G, Schrader J (2001) Inotropic response to beta-adrenergic receptor stimulation and anti-adrenergic effect of ACh in endothelial NO synthase-deficient mouse hearts. J Physiol 532:195–204. doi:10.1111/j.1469-7793.2001.0195g.x
39. Gonzalez DR, Beigi F, Treuer AV, Hare JM (2007) Deficient ryanodine receptor S-nitrosylation increases sarcoplasmic reticulum calcium leak and arrhythmogenesis in cardiomyocytes. Proc Natl Acad Sci USA 104:20612–20617. doi:10.1073/pnas.0706796104
40. Gorressen S, Stern M, van de Sandt AM, Cortese-Krott MM, Ohlig J, Rassaf T, Gödecke A, Fischer JW, Heusch G, Merx MW, Kelm M (2015) Circulating NOS3 modulates left ventricular remodeling following reperfused myocardial infarction. PLoS One 10:e0120961. doi:10.1371/journal.pone.0120961
41. Gupte SA, Okada T (2001) Prostaglandins and nitric oxide mediate superoxide-induced myocardial contractile dysfunction in isolated rat hearts. J Mol Cell Cardiol 33:1107–1117. doi:10.1006/jmcc.2001.1371
42. Hayashi T, Arimura T, Ueda K, Shibata H, Hohda S, Takahashi M, Hori H, Koga Y, Oka N, Imaizumi T, Yasunami M, Kimura A (2004) Identification and functional analysis of a caveolin-3 mutation associated with familial hypertrophic cardiomyopathy. Biochem Biophys Res Commun 313:178–184. doi:10.1016/j.bbrc.2003.11.101

43. Hayashi YK, Matsuda C, Ogawa M, Goto K, Tominaga K, Mitsuhashi S, Park YE, Nonaka I, Hino-Fukuyo N, Haginoya K, Sugano H, Nishino I (2009) Human PTRF mutations cause secondary deficiency of caveolins resulting in muscular dystrophy with generalized lipodystrophy. J Clin Invest 119:2623–2633. doi:10.1172/Jci38660
44. Heinzel FR, Gres P, Boengler K, Duschin A, Konietzka I, Rassaf T, Snedovskaya J, Meyer S, Skyschally A, Kelm M, Heusch G, Schulz R (2008) Inducible nitric oxide synthase expression and cardiomyocyte dysfunction during sustained moderate ischemia in pigs. Circ Res 103:1120–1127. doi:10.1161/CIRCRESAHA.108.186015
45. Heusch G, Post H, Michel MC, Kelm M, Schulz R (2000) Endogenous nitric oxide and myocardial adaptation to ischemia. Circ Res 87:146–152 **PMID: 10903999**
46. Hill MM, Bastiani M, Luetterforst R, Kirkham M, Kirkham A, Nixon SJ, Walser P, Abankwa D, Oorschot VM, Martin S, Hancock JF, Parton RG (2008) PTRF-Cavin, a conserved cytoplasmic protein required for caveola formation and function. Cell 132:113–124. doi:10.1016/j.cell.2007.11.042
47. Horikawa YT, Patel HH, Tsutsumi YM, Jennings MM, Kidd MW, Hagiwara Y, Ishikawa Y, Insel PA, Roth DM (2008) Caveolin-3 expression and caveolae are required for isoflurane-induced cardiac protection from hypoxia and ischemia/reperfusion injury. J Mol Cell Cardiol 44:123–130. doi:10.1016/j.yjmcc.2007.10.003
48. Hu A, Jiao X, Gao E, Koch WJ, Sharifi-Azad S, Grunwald Z, Ma XL, Sun JZ (2006) Chronic beta-adrenergic receptor stimulation induces cardiac apoptosis and aggravates myocardial ischemia/reperfusion injury by provoking inducible nitric-oxide synthase-mediated nitrative stress. J Pharmacol Exp Ther 318:469–475. doi:10.1124/jpet.106.102160
49. Israeli-Rosenberg S, Chen C, Li R, Deussen DN, Niesman IR, Okada H, Patel HH, Roth DM, Ross RS (2015) Caveolin modulates integrin function and mechanical activation in the cardiomyocyte. FASEB J 29:374–384. doi:10.1096/fj.13-243139
50. Jansa P, Mason SW, Hoffmann-Rohrer U, Grummt I (1998) Cloning and functional characterization of PTRF, a novel protein which induces dissociation of paused ternary transcription complexes. EMBO J 17:2855–2864. doi:10.1093/emboj/17.10.2855
51. Jasmin JF, Rengo G, Lymperopoulos A, Gupta R, Eaton GJ, Quann K, Gonzales DM, Mercier I, Koch WJ, Lisanti M (2011) Caveolin-1 deficiency exacerbates cardiac dysfunction and reduces survival in mice with myocardial infarction. Am J Physiol Heart Circ Physiol 300:H1274–H1281. doi:10.1152/ajpheart.01173.2010
52. Karbalaei MS, Rippe C, Albinsson S, Ekman M, Mansten A, Uvelius B, Swärd K (2012) Impaired contractility and detrusor hypertrophy in cavin-1-deficient mice. Eur J Pharmacol 689:179–185. doi:10.1016/j.ejphar.2012.05.023
53. Kingma I, Smiseth OA, Belenkie I, Knudtson ML, MacDonald RP, Tyberg JV, Smith ER (1986) A mechanism for the nitroglycerin-induced downward shift of the left ventricular diastolic pressure–diameter relationship of patients. Am J Cardiol 57:673–677. doi:10.1016/0002-9149(86)90857-X
54. Kinugawa K, Takahashi T, Kohmoto O, Yao A, Aoyagi T, Momomura S, Hirata Y, Serizawa T (1994) Nitric oxide-mediated effects of interleukin-6 on $[Ca^{2+}]_i$ and cell contraction in cultured chick ventricular myocytes. Circ Res 75:285–295. doi:10.1161/01.RES.75.2.285
55. Klabunde RE, Kimber ND, Kuk JE, Helgren MC, Förstermann U (1992) N^G-Methyl-L-arginine decreases contractility, cGMP and cAMP in isoproterenol-stimulated rat hearts in vitro. Eur J Pharmacol 223:1–7. doi:10.1016/0014-2999(92)90810-Q
56. Kovtun O, Tillu VA, Jung W, Leneva N, Ariotti N, Chaudhary N, Mandyam RA, Ferguson C, Morgan GP, Johnston WA, Harrop SJ, Alexandrov K, Parton RG, Collins BM (2014) Structural insights into the organization of the cavin membrane coat complex. Dev Cell 31:405–419. doi:10.1016/j.devcel.2014.10.002
57. Liu L, Brown D, McKee M, Lebrasseur NK, Yang D, Albrecht KH, Ravid K, Pilch PF (2008) Deletion of Cavin/PTRF causes global loss of caveolae, dyslipidemia, and glucose intolerance. Cell Metab 8:310–317. doi:10.1016/j.cmet.2008.07.00
58. Lo HP, Nixon SJ, Hall TE, Cowling BS, Ferguson C, Morgan GP, Schieber NL, Fernandez-Rojo MA, Bastiani M, Floetenmeyer M, Martel N, Laporte J, Pilch PF, Parton RG (2015) The caveolin-cavin system plays a conserved and critical role in mechanoprotection of skeletal muscle. J Cell Biol 210:833–849. doi:10.1083/jcb.201501046
59. Lu XM, Zhang GX, Yu YQ, Kimura S, Nishiyama A, Matsuyoshi H, Shimizu J, Takaki M (2009) The opposite roles of nNOS in cardiac ischemia-reperfusion-induced injury and in ischemia preconditioning-induced cardioprotection in mice. J Physiol Sci 59:253–262. doi:10.1007/s12576-009-0030-1
60. Mankad P, Yacoub M (1997) Influence of basal release of nitric oxide on systolic and diastolic function of both ventricles. J Thorac Cardiovasc Surg 113:770–776. doi:10.1016/S0022-5223(97)70236-8
61. Martin C, Schulz R, Post H, Gres P, Heusch G (2003) Effect of NO synthase inhibition on myocardial metabolism during moderate ischemia. Am J Physiol Heart Circ Physiol 284:H2320–H2324. doi:10.1152/ajpheart.01122.2002
62. Martin C, Schulz R, Post H, Boengler K, Kelm M, Kleinbongard P, Gres P, Skyschally A, Konietzka I, Heusch G (2007) Microdialysis-based analysis of interstitial NO in situ: NO synthase-independent NO formation during myocardial ischemia. Cardiovasc Res 74:46–55. doi:10.1016/j.cardiores.2006.12.020
63. Matheis G, Sherman MP, Buckberg GD, Haybron DM, Young HH, Ignarro LJ (1992) Role of L-arginine-nitric oxide pathway in myocardial reoxygenation injury. Am J Physiol 262:H616–H620 **PMID: 1539723**
64. Merx MW, Gorressen S, van de Sandt AM, Cortese-Krott MM, Ohlig J, Stern M, Rassaf T, Gödecke A, Gladwin MT, Kelm M (2014) Depletion of circulating blood NOS3 increases severity of myocardial infarction and left ventricular dysfunction. Basic Res Cardiol 109:398. doi:10.1007/s00395-013-0398-1
65. Michel JB, Feron O, Sacks D, Michel T (1997) Reciprocal regulation of endothelial nitric-oxide synthase by Ca^{2+}-calmodulin and caveolin. J Biol Chem 272:15583–15586. doi:10.1074/jbc.272.25.15583
66. Murata T, Lin MI, Huang Y, Yu J, Bauer PM, Giordano FJ, Sessa WC (2007) Re-expression of caveolin-1 in endothelium rescues the vascular, cardiac, and pulmonary defects in global caveolin-1 knockout mice. J Exp Med 204:2373–2382. doi:10.1084/jem.20062340
67. Ohsawa Y, Toko H, Katsura M, Morimoto K, Yamada H, Ichikawa Y, Murakami T, Ohkuma S, Komuro I, Sunada Y (2004) Overexpression of P104L mutant caveolin-3 in mice develops hypertrophic cardiomyopathy with enhanced contractility in association with increased endothelial nitric oxide synthase activity. Hum Mol Genet 13:151–157. doi:10.1093/hmg/ddh014
68. Park KH, Rubin LE, Gross SS, Levi R (1992) Nitric oxide is a mediator of hypoxic coronary vasodilatation. Relation to adenosine and cyclooxygenase-derived metabolites. Circ Res 71:992–1001. doi:10.1161/01.RES.71.4.992
69. Patel HH, Tsutsumi YM, Head BP, Niesman IR, Jennings M, Horikawa Y, Huang D, Moreno AL, Patel PM, Insel PA, Roth

DM (2007) Mechanisms of cardiac protection from ischemia/reperfusion injury: a role for caveolae and caveolin-1. FASEB J 21:1565–1574. doi:10.1096/fj.06-7719com
70. Parton RG, del Pozo MA (2013) Caveolae as plasma membrane sensors, protectors and organizers. Nat Rev Mol Cell Biol 14:98–112. doi:10.1083/jcb.201501046
71. Paulus WJ, Shah AM (1999) NO and cardiac diastolic function. Cardiovasc Res 43:595–606. doi:10.1016/S0008-6363(99)00151-0
72. Post H, d'Agostino C, Lionetti V, Castellari M, Kang EY, Altarejos M, Xu X, Hintze TH, Recchia FA (2003) Reduced left ventricular compliance and mechanical efficiency after prolonged inhibition of NO synthesis in conscious dogs. J Physiol 552:233–239. doi:10.1113/jphysiol.2003.048769
73. Post H, Schulz R, Behrends M, Gres P, Umschlag C, Heusch G (2000) No involvement of endogenous nitric oxide in classical ischemic preconditioning in swine. J Mol Cell Cardiol 32(5):725–733. doi:10.1006/jmcc.2000.1117
74. Post H, Schulz R, Gres P, Heusch G (2001) No involvement of nitric oxide in the limitation of beta-adrenergic inotropic responsiveness during ischemia. Am J Physiol Heart Circ Physiol 281:H2392–H2397
75. Prendergast BD, Sagach VF, Shah AM (1997) Basal release of nitric oxide augments the Frank-Starling response in the isolated heart. Circulation 96:1320–1329. doi:10.1161/01.CIR.96.4.1320
76. Puybasset L, Béa ML, Ghaleb B, Giudicelli JF, Berdeaux A (1996) Coronary and systemic hemodynamic effects of sustained inhibition of nitric oxide synthesis in conscious dogs. Evidence for cross talk between nitric oxide and cyclooxygenase in coronary vessels. Circ Res 79:343–357. doi:10.1161/01.RES.79.2.343
77. Rajab A, Straub V, McCann LJ, Seelow D, Varon R, Barresi R, Schulze A, Lucke B, Lützkendorf S, Karbasiyan M, Bachmann S, Spuler S, Schuelke M (2010) Fatal cardiac arrhythmia and long-QT syndrome in a new form of congenital generalized lipodystrophy with muscle rippling (CGL4) due to PTRF-CAVIN mutations. PLoS Genet 6:e1000874. doi:10.1371/journal.pgen.1000874
78. Rassaf T, Kleinbongard P, Preik M, Dejam A, Gharini P, Lauer T, Erckenbrecht J, Duschin A, Schulz R, Heusch G, Feelisch M, Kelm M (2002) Plasma nitrosothiols contribute to the systemic vasodilator effects of intravenously applied NO: experimental and clinical Study on the fate of NO in human blood. Circ Res 91:470–477 **PMID: 12242264**
79. Rassaf T, Totzeck M, Hendgen-Cotta UB, Shiva S, Heusch G, Kelm M (2014) Circulating nitrite contributes to cardioprotection by remote ischemic preconditioning. Circ Res 9:1601–1610. doi:10.1161/CIRCRESAHA.114.303822
80. Razani B, Engelman JA, Wang XB, Schubert W, Zhang XL, Marks CB, Macaluso F, Russell RG, Li M, Pestell RG, Di Vizio D, Hou H Jr, Kneitz B, Lagaud G, Christ GJ, Edelmann W, Lisanti MP (2001) Caveolin-1 null mice are viable but show evidence of hyperproliferative and vascular abnormalities. J Biol Chem 276:38121–38138. doi:10.1074/jbc.M105408200
81. Reichelt ME, Willems L, Hack BA, Peart JN, Headrick JP (2009) Cardiac and coronary function in the Langendorff-perfused mouse heart model. Exp Physiol 94:54–70. doi:10.1113/expphysiol.2008.043554
82. Rizzo V, McIntosh DP, Oh P, Schnitzer JE (1998) In situ flow activates endothelial nitric oxide synthase in luminal caveolae of endothelium with rapid caveolin dissociation and calmodulin association. J Biol Chem 273:34724–34729. doi:10.1074/jbc.273.52.34724
83. Rodriguez G, Ueyama T, Ogata T, Czernuszewicz G, Tan Y, Dorn GW 2nd, Bogaev R, Amano K, Oh H, Matsubara H, Willerson JT, Marian AJ (2011) Molecular genetic and functional characterization implicate muscle-restricted coiled-coil gene (MURC) as a causal gene for familial dilated cardiomyopathy. Circ Cardiovasc Genet 4:349–358. doi:10.1161/CIRCGENETICS.111.959866
84. Schilling JM, Roth DM, Patel HH (2015) Caveolins in cardioprotection—translatability and mechanisms. Br J Pharmacol 172:2114–2125. doi:10.1111/bph.13009
85. Schilling JM, Horikawa YT, Zemljic-Harpf AE, Vincent KP, Tyan L, Yu JK, McCulloch AD, Balijepalli RC, Patel HH, Roth DM (2016) Electrophysiology and metabolism of caveolin-3-overexpressing mice. Basic Res Cardiol 111:28. doi:10.1007/s00395-016-0542-9
86. Schulz R, Wambolt R (1995) Inhibition of nitric oxide synthesis protects the isolated working rabbit heart from ischemia-reperfusion injury. Cardiovasc Res 30:432–439. doi:10.1016/S0008-6363(95)00064-X
87. Schulz R, Kelm M, Heusch G (2004) Nitric oxide in myocardial ischemia/reperfusion injury. Cardiovasc Res 61:402–413. doi:10.1016/j.cardiores.2003.09.019
88. See Hoe LE, Schilling JM, Tarbit E, Kiessling CJ, Busija AR, Niesman IR, Du Toit E, Ashton KJ, Roth DM, Headrick JP, Patel HH, Peart JN (2014) Sarcolemmal cholesterol and caveolin-3 dependence of cardiac function, ischemic tolerance, and opioidergic cardioprotection. Am J Physiol Heart Circ Physiol 307:H895–H903. doi:10.1152/ajpheart.00081.2014
89. Smith RE, Palmer RM, Bucknall CA, Moncada S (1992) Role of nitric oxide synthesis in the regulation of coronary vascular tone in the isolated perfused rabbit heart. Cardiovasc Res 26:508–512. doi:10.1093/cvr/26.5.508
90. Song DW, Lee KE, Ryu JY, Jeon H, Kim Do H (2015) The molecular interaction of heart LIM protein (HLP) with RyR2 and caveolin-3 is essential for Ca^{2+}-induced Ca^{2+} release in the heart. Biochem Biophys Res Commun 463:975–981. doi:10.1016/j.bbrc.2015.06.045
91. Swärd K, Albinsson S, Rippe C (2014) Arterial dysfunction but maintained systemic blood pressure in cavin-1-deficient mice. PLoS One 9:e92428. doi:10.1371/journal.pone.0092428
92. Swärd K, Sadegh MK, Mori M, Erjefält JS, Rippe C (2013) Elevated pulmonary arterial pressure and altered expression of Ddah1 and Arg1 in mice lacking cavin-1/PTRF. Physiol Rep 1:e00008. doi:10.1002/PHY2.8
93. Takasato M, Er PX, Chiu HS, Maier B, Baillie GJ, Ferguson C, Parton RG, Wolvetang EJ, Roost MS, de Sousa Chuva, Lopes SM, Little MH (2015) Kidney organoids from human iPS cells contain multiple lineages and model human nephrogenesis. Nature 526:564–568. doi:10.1038/nature15695
94. Taniguchi T, Maruyama N, Ogata T, Kasahara T, Nakanishi N, Miyagawa K, Naito D, Hamaoka T, Nishi M, Matoba S, Ueyama T (2016) PTRF/Cavin-1 deficiency causes cardiac dysfunction accompanied by cardiomyocyte hypertrophy and cardiac fibrosis. PLoS One 11:e0162513. doi:10.1371/journal.pone.0162513
95. Tsutsumi YM, Horikawa YT, Jennings MM, Kidd MW, Niesman IR, Yokoyama U, Head BP, Hagiwara Y, Ishikawa Y, Miyanohara A, Patel PM, Insel PA, Patel HH, Roth DM (2008) Cardiac- specific overexpression of caveolin-3 induces endogenous cardiac protection by mimicking ischemic preconditioning. Circulation 118:1979–1988. doi:10.1161/CIRCULATIONAHA.108.788331
96. Tune JD, Richmond KN, Gorman MW, Feigl EO (2000) Role of nitric oxide and adenosine in control of coronary blood flow in exercising dogs. Circulation 101:2942–2948. doi:10.1161/01.CIR.101.25.2942
97. Ueeda M, Silvia SK, Olsson RA (1992) Nitric oxide modulates coronary autoregulation in the guinea pig. Circ Res 70:1296–1303. doi:10.1161/01.RES.70.6.1296

98. Vatta M, Ackerman MJ, Ye B, Makielski JC, Ughanze EE, Taylor EW, Tester DJ, Balijepalli RC, Foell JD, Li Z, Kamp TJ, Towbin JA (2006) Mutant caveolin-3 induces persistent late sodium current and is associated with long-QT syndrome. Circulation 114:2104–2112. doi:10.1161/CIRCULATIONAHA.106.635268
99. Vila-Petroff MG, Kim SH, Pepe S, Dessy C, Marban E, Balligand JL, Sollott SJ (2001) Endogenous nitric oxide mechanisms mediate the stretch dependence of Ca^{2+} release in cardiomyocytes. Nat Cell Biol 3:867–873. doi:10.1038/ncb1001-867
100. Volonte D, Galbiati F (2011) Polymerase I and transcript release factor (PTRF)/cavin-1 is a novel regulator of stress-induced premature senescence. J Biol Chem 286:28657–28661. doi:10.1074/jbc.C111.235119
101. Walsh EK, Huang H, Wang Z, Williams J, de Crom R, van Haperen R, Thompson CI, Lefer DJ, Hintze TH (2004) Control of myocardial oxygen consumption in transgenic mice overexpressing vascular eNOS. Am J Physiol Heart Circ Physiol 287:H2115–H2121. doi:10.1152/ajpheart.00267.2004
102. Wang D, Yang XP, Liu YH, Carretero OA, LaPointe MC (1999) Reduction of myocardial infarct size by inhibition of inducible nitric oxide synthase. Am J Hypertens 12:174–182. doi:10.1016/S0895-7061(98)00235-0
103. Wang H, Kohr MJ, Traynham CJ, Wheeler DG, Janssen PM, Ziolo MT (2008) Neuronal nitric oxide synthase signaling within cardiac myocytes targets phospholamban. Am J Physiol Cell Physiol 294:C1566–C1575. doi:10.1152/ajpcell.00367.2007
104. Wang P, Zweier JL (1996) Measurement of nitric oxide and peroxynitrite generation in the postischemic heart. Evidence for peroxynitrite-mediated reperfusion injury. J Biol Chem 271:29223–29230. doi:10.1074/jbc.271.46.29223
105. Whiteley G, Collins RF, Kitmitto A (2012) Characterization of the molecular architecture of human caveolin-3 and interaction with the skeletal muscle ryanodine receptor. J Biol Chem 287:40302–40316. doi:10.1074/jbc.M112.377085
106. Wildhirt SM, Suzuki H, Horstman D, Weismüller S, Dudek RR, Akiyama K, Reichart B (1997) Selective modulation of inducible nitric oxide synthase isoenzyme in myocardial infarction. Circulation 96:1616–1623. doi:10.1161/01.CIR.96.5.1616
107. Woodman SE, Park DS, Cohen AW, Cheung MW, Chandra M, Shirani J, Tang B, Jelicks LA, Kitsis RN, Christ GJ, Factor SM, Tanowitz HB, Lisanti MP (2002) Caveolin-3 knock-out mice develop a progressive cardiomyopathy and show hyperactivation of the p42/44 MAPK cascade. J Biol Chem 277:38988–38997. doi:10.1074/jbc.M205511200
108. Wunderlich C, Schober K, Kasper M, Heerwagen C, Marquetant R, Ebner B, Forkmann M, Schoen S, Braun-Dullaeus RC, Schmeisser A, Strasser RH (2008) Nitric oxide synthases are crucially involved in the development of the severe cardiomyopathy of caveolin-1 knockout mice. Biochem Biophys Res Commun 377:769–774. doi:10.1016/j.bbrc.2008.10.068
109. Xu L, Eu JP, Meissner G, Stamler JS (1998) Activation of the cardiac calcium release channel (ryanodine receptor) by poly-S-nitrosylation. Science 279:234–237. doi:10.1126/science.279.5348.234
110. Xu KY, Huso DL, Dawson TM, Bredt DS, Becker LC (1999) Nitric oxide synthase in cardiac sarcoplasmic reticulum. Proc Natl Acad Sci USA 96:657–662. doi:10.1073/pnas.96.2.657
111. Yang Y, Ma Z, Hu W, Wang D, Jiang S, Fan C, Di S, Liu D, Sun Y, Yi W (2016) Caveolin-1/-3: therapeutic targets for myocardial ischemia/reperfusion injury. Basic Res Cardiol 111:45. doi:10.1007/s00395-016-0561-6
112. Yu J, Bergaya S, Murata T, Alp IF, Bauer MP, Lin MI, Drab M, Kurzchalia TV, Stan RV, Sessa WC (2006) Direct evidence for the role of caveolin-1 and caveolae in mechanotransduction and remodeling of blood vessels. J Clin Invest 116:1284–1291. doi:10.1172/JCI27100
113. Zatta AJ, Headrick JP (2005) Mediators of coronary reactive hyperaemia in isolated mouse heart. Br J Pharmacol 144:576–587. doi:10.1038/sj.bjp.0706099
114. Zhao YY, Liu Y, Stan RV, Fan L, Gu Y, Dalton N, Chu PH, Peterson K, Ross J Jr, Chien KR (2002) Defects in caveolin-1 cause dilated cardiomyopathy and pulmonary hypertension in knockout mice. Proc Natl Acad Sci USA 99:11375–11380. doi:10.1073/pnas.172360799
115. Zhao X, Chen YR, He G, Zhang A, Druhan LJ, Strauch AR, Zweier JL (2007) Endothelial nitric oxide synthase (NOS3) knockout decreases NOS2 induction, limiting hyperoxygenation and conferring protection in the postischemic heart. Am J Physiol Heart Circ Physiol 292:H1541–H1550. doi:10.1152/ajpheart.00264.2006
116. Zhou L, Burnett AL, Huang PL, Becker LC, Kuppusamy P, Kass DA, Kevin Donahue J, Proud D, Sham JS, Dawson TM, Xu KY (2002) Lack of nitric oxide synthase depresses ion transporting enzyme function in cardiac muscle. Biochem Biophys Res Commun 294:1030–1035. doi:10.1016/S0006-291X(02)00599-5
117. Zhu H, Lin P, De G, Choi KH, Takeshima H, Weisleder N, Ma J (2011) Polymerase transcriptase release factor (PTRF) anchors MG53 protein to cell injury site for initiation of membrane repair. J Biol Chem 286:12820–12824. doi:10.1074/jbc.C111.22144093